Spectroscopic measurements of the cold component of electron in Ion Cyclotron Heating Experiments on RT-1 plasma

47-146073

Kashyap Ankur

Master's Thesis

Submitted in February 2016

Academic Supervisor: Professor Yoshida Zensho

The University Of Tokyo
Graduate School Of Frontier Sciences
Department Of Advanced Energy

Contents

Abstract **iv**

1 Introduction **1**

1.1 Magneto-spheric confinement of High temperature plasma 1

1.2 Two component electrons 3

1.3 Objective 7

2 Spectroscopic Measurement **9**

2.1 Helium line intensity ratio method 9

2.2 Collisional Radiative model 22

2.3 Abel Transform 26

3 Experimental setup **31**

3.1 Ring Trap 1, the artificial magnetosphere 31

3.2 Diagnostic and measurement systems in RT-1 33

3.3 Spectroscopic System 37

3.4 Experimental Setup 40

4 Density and temperature profile **44**

4.1 Data fitting 44

4.2 Density and temperature profile in case of levitation 46

4.3 Density and temperature profile in case of support 54

4.4 Discussion 62

5 Conclusion **66**

6 Appendix **69**

7 Scientific Meetings **84**

8 Acknowledgment **86**

Abstract

The laboratory magnetosphere, RT-1, confines extremely $high\beta$ plasma in a dipole magnetic configuration, generated by levitating a super conducting coil. The main constituents of the confined plasma are ions and two components of electrons-the hot component and the cold component; typically, both the components have comparable fractions. The electron density profile of the hot component of electron has been interpolated with the help of the line averaged densities obtained from interferometry, and the temperature of the hot component of electron has been measured to be around 10∼50 keV. However, temperature and density profiles of the cold component of electron has yet not been measured. The hot component of electron due to it‘s high energies does not interact with ions. The cold component of electron is supposed to be interacting with ions, and could be responsible for heating up ions. More recent experiments with Ion Cyclotron Heating (ICH) have shown the heating of ions as well as the cold component of electron due to ICH- during levitation . However, whether the cold component of electron is getting heated indirectly by ICH through ions or directly by ICH, is yet not known. Therefore, in order to delineate the whole heating mechanism, the information about the density and temperature profile of the cold component in RT-1 plasma becomes increasingly pertinent. The temperature and density profile of the cold component of electron, in this research, have been estimated using helium I line intensity ratio method, and a pair of line intensity ratios- one sensitive to electron temperature and other sensitive to the electron density- have been used in concert to find the self-consistent solution, both for electron

temperature and density. Calculated results are then compared with the results obtained by probe measurements and interferometry. Comparison between the temperature of the cold component of electrons and ion‘s temperature are also performed.

Chapter 1

Introduction

1.1 Magneto-spheric confinement of High temperature plasma

Ring trap (RT-1) is a laboratory magnetosphere device that confines ultra highβplasma in a dipole magnetic configuration generated by levitating a superconducting coil- which is made of Bi-223 alloy- as shown in figure 1.1.The superconducting coil is levitated by interactions with an electromagnet situated at the top of RT-1. The plasma inside RT-1 is created primarily with Electron Cyclotron Resonance Heating(ECRH)with 8.2 and 2.45 GHz microwaves and ,more recently, Ion Cyclotron Resonance Heating(ICRH)in concert with ECRH. RT-1 was constructed mainly to study the peculiar phenomenon of plasma confinement in a dipole magnetic configuration-which is the most frequently occurring magnetic

configuration in the universe, and to achieve a high performance plasma confinement in an artificially generated dipole magnetic confinement.The effects of the flow and interaction with a strong inhomogeneous dipole magnetic field are considered to be important factors giving rise to extremely stable plasma confinement properties.Furthermore,the ultra highβ plasma configuration- achieved successfully in RT-1-could make advanced nuclear fusion using D-D and D-^3He fuels possible in the future. For the aforementioned reasons, experiments on RT-1 using dipole magnetic configuration have become increasingly important.

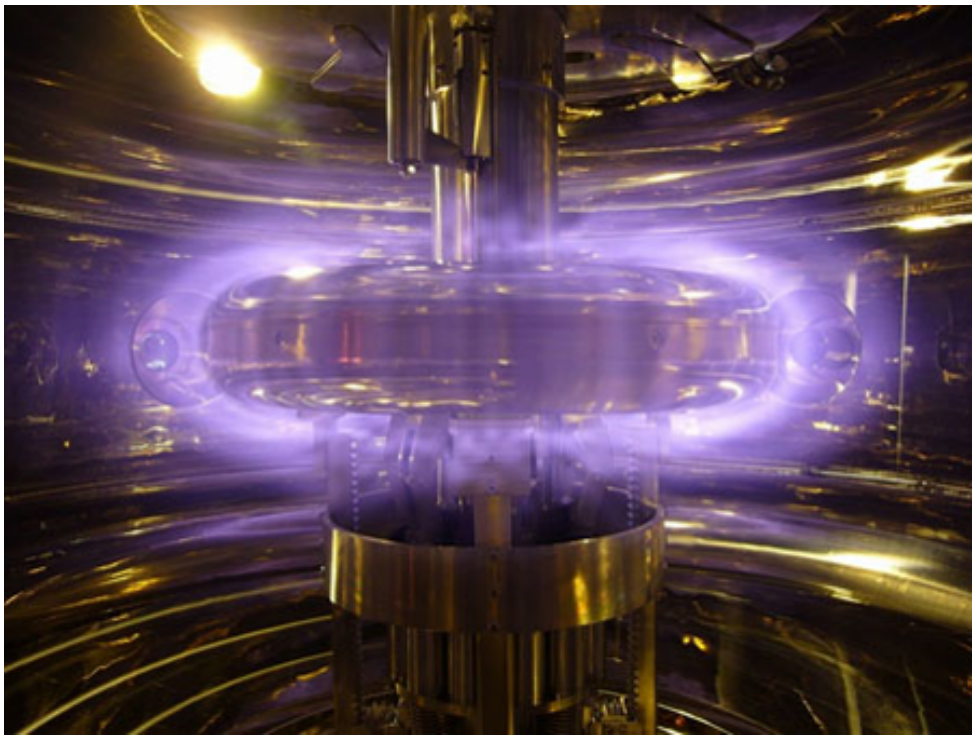

Figure 1.1: Inside view of RT-1 showing the levitated coil during a plasma discharge.Figure of [1]

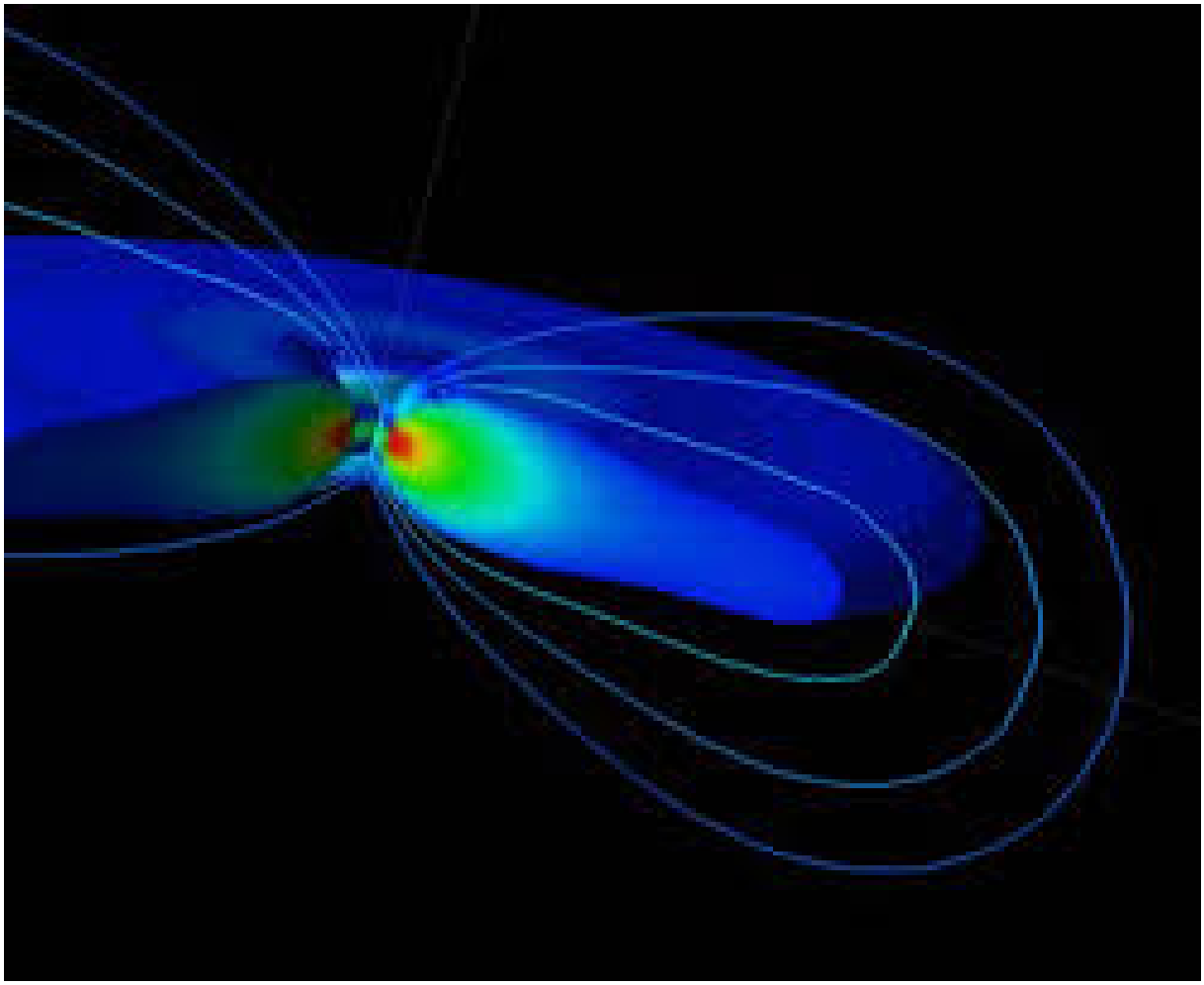

Figure 1.2: Planetary dipole magnetic configuration of planet Jupiter. Figure 1 of [2]

1.2 Two component electrons

The plasmas confined in RT-1 mainly consist of ions, hot component of electrons,cold component of electron and neutral atoms. The properties of the hot component of electron have been studied very comprehensively in RT-1 plasma. The density profile of the hot component of electron has successfully been interpolated by using a three pair chord

interferometry as shown in figure 1.2[H˙saitoh]. Soft x-ray measurements by a Si(Li) detector estimate the temperature of the hot component of electron to be around 10keV, as can be seen from the figure 1.3. Although, the edge Langmuir probe measurements have shown the presence of cold electron($T_{cold} \approx 10eV$). More recently, the temperature

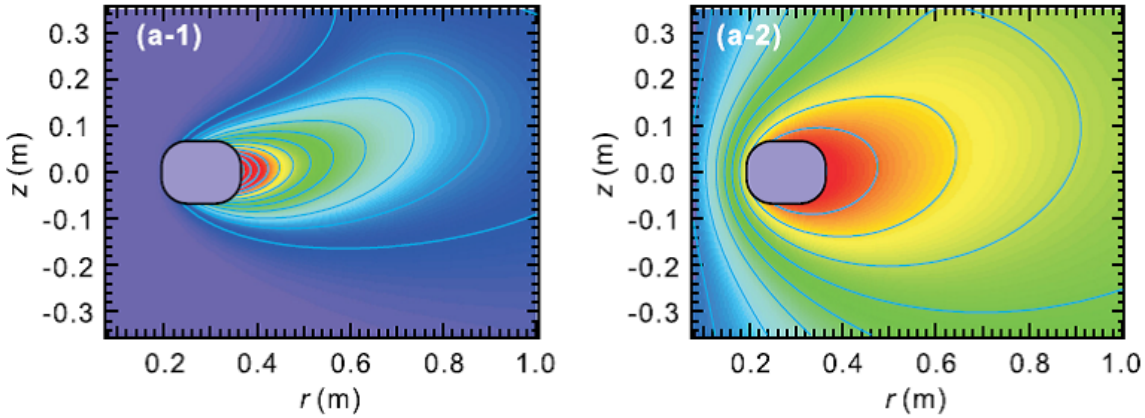

Figure 1.3: Reconstructed total electron density profile for a-1) 2.5mPa and a-2)15 mPa[2]. Figure of [3]

profile of ion() inside RT-1 plasma has also been estimated by observing the Doppler effect for helium ions, as can be seen from the figure below.

However, a comprehensive study regarding the temperature and density distribution of the cold component of of electron has not yet been performed. The cold component of electron is considered to play an important role in the energy balance of ions inside RT-1 plasma, and therefore it is essential to obtain the temperature and density profile of the cold component of electrons inside RT-1.As mentioned earlier, electrons in RT-1 plasmas consist of two species,the hot component and the cold component.The hot component of

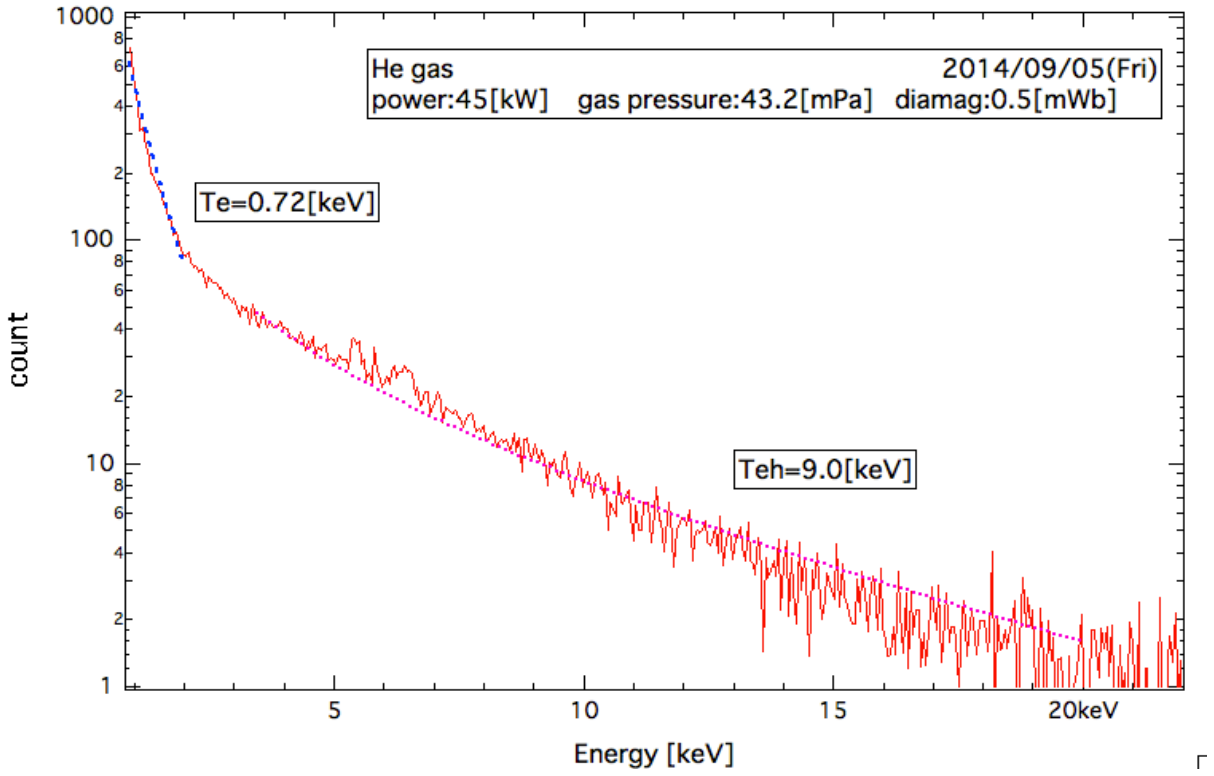

Figure 1.4: Soft X-ray spectrum used for the determination of the hot component of electron[4]

electron, due to extremely high energies, do not couple with ions inside RT-1 plasma. It is only the cold component of electron, which because of their low energies, can interact with ions through coulomb collision, and may be responsible for heating the ions up. More recently, the heating of the cold component of electron by Ion Cyclotron Resonance Heating (ICRH) waves-generated by the newly installed ICRH antenna- has been observed in RT-1 plasma during levitation. However, the mechanism of the heating process is yet unknown, and further investigation is required. For the above mentioned reasons, the estimation of the density and temperature profile of the cold component of electrons has

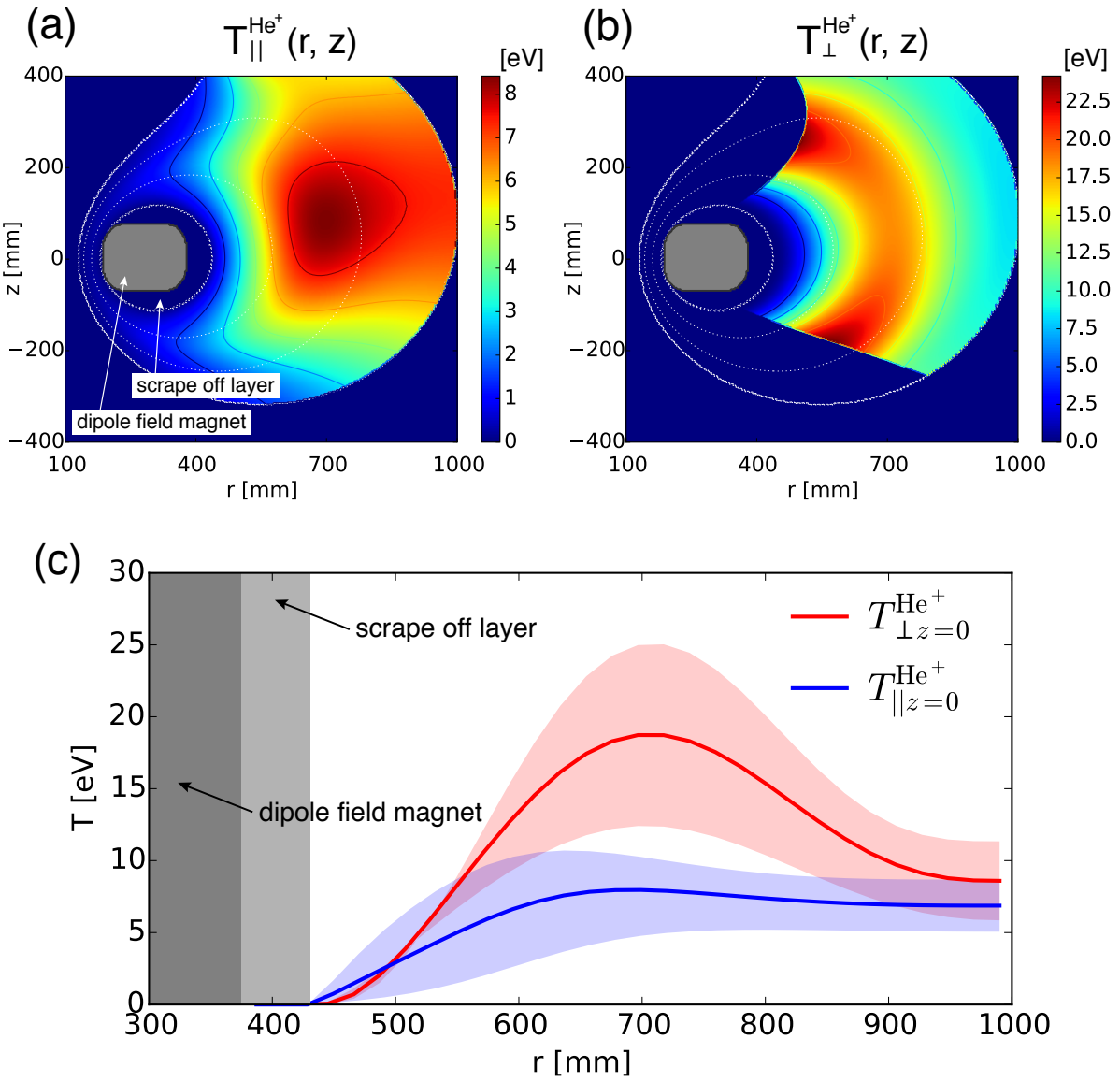

Figure 1.5: Poloidal(r-z plane)cross-section of a)$T_{||}$ component b)$T_{\perp}$component c)radial profiles $T_{||}$ and$T_{\perp}$ for z= ofHe^+ inside RT-1 plasma for levitated coil.Fig.2 of [5]

become increasingly important.

1.3 Objective

In this research,we employ a spectroscopic technique known as Helium line intensity ratio method to estimate the density and temperature profile of the cold component of electron. As has been mentioned before, the Langmuir probe measurements at the edge of RT-1 found the temperature of the cold component of electrons to be around 10eV. The temperature of the hot component of electron increases tremendously as one approaches the central region of RT-1, which precludes any direct measurement of that region by probe insertion. Passive spectroscopy - used in this research- is a cheap and efficient way to diagnose the hot interior of RT-1 plasma indirectly. Firstly, intensities of the required helium I spectral lines-emanated from the plasma inside RT-1- are measured spectroscopically. Intensity ratios from the suitable pair of spectral lines are calculated, and are then used together with the Abel Transform model constructed in this research to obtain the density and temperature profile of the cold component of electron inside RT-1. Then, we observe the heating effects of ICH on the cold component of electron. Finally. the temperature and the density profiles for both- Ion Cyclotron Resonance Heating on and off- scenarios are calculated. In this thesis, first we discuss the theoretical model on which this research is predicated; i.e, helium line intensity ratio method, collisional radiative model that was used to calculate the population densities of the respective

emanating energy levels of the neutral helium atom, and the Abel Transform formulation that yielded us the density and temperature profile of the cold component of electrons.In the next section, the experimental set-up and procedure for the data analysis are discussed. The following section after that covers the results obtained:the density and temperature profiles of the cold component of electrons both for levitated and non-levitated cases and comparisons with other modes of measurements such as interferometry and probe measurements have been reported.In the last section, the conclusion of our results and areas with the possible scope of improvement are discussed briefly.

Chapter 2

Spectroscopic measurement of the cold component of electron

2.1 Helium line intensity ratio method

In this research, we have employed Helium Line intensity ratio method for the determination of temperature and density of the cold component of electron.The temperature of hot electrons inside the central region of RT-1 has been found to be around 10 KeV, which makes any measurements at the central region by probe insertion impossible, and thereby limiting the diagnostics by probe only to the periphery of RT-1. The measurement by probe diagnostics does not provide the complete density and temperature profiles of RT-1. Passive spectroscopy is quite suitable for aforementioned purpose as it does not require direct insertion of any device inside the extremely hot plasma. In this research,

we measured the line intensities of neutral helium emitted by RT-1 plasma through a collimator, and applied Abel inversion to the ratios of the measured line integrated intensities to get the spatial profiles of the temperature and density for the cold component of electrons inside RT-1.

The line intensity ratio diagnostic is based on the fact that under a certain density regime, ratio of a pair spectral lines is exclusively either a strong function of electron temperature or a strong function of electron density. A spectral line intensity ratio which depends strongly on electron temperature and weakly on electron density can be used to find the electron temperature of plasma, and similarly, a line ratio,which is a strong function of electron density and depends very slightly on electron temperature, can be used to calculate the electron density of plasma. Here, we have used the line intensity ratios sensitive to electron temperature in concord with the intensity ratios sensitive to electron density, and applied Abel transform to calculate the temperature and density profiles of the cold component of electrons inside RT-1 plasma. Below is a brief theoretical formulation of the intensity line ratio diagnostic method. The plasma emits radiation which is collected using a collimator and fed into spectrometer through an optical fibre. The plasma emissivity ε_{ij}(W/vol·solid angle)for a specific wavelength λ_{ij} corresponding to a transition from excited level i to j, can be written as

$$\varepsilon_{ij} = (4\Pi)^{-1} h\nu_{ij} N_i A_{ij} \tag{2.1}$$

where $h\nu_{ij}$ is the photon energy, N_i is the population density of the energy level from where the line originates,A_{ij} is the Einstein coefficient for the transition. If we assume the plasma is uniform, the photon count rate $I_p(\lambda_{ij})$measured by the CCD camera at wavelength λ_{ij} is given by:

$$I_p(\lambda_{ij}) = (4\Pi)^{-1} N_i A_{ij}\, V\Omega\, T(\lambda_{ij})\eta(\lambda_{ij}) \tag{2.2}$$

where V is the volume of the plasma seen by the monochromator,Ω is the solid angle subtended by the collimator(collection optics system), $T(\lambda_{ij})$ is the transmission factor of the detection system, and $\eta(\lambda_{ij})$ is the CCD camera quantum efficiency at wavelengthλ_{ij}. The ratio of the photon count for two lines of wavelength λ_{ij} andλ_{kl} can be written as

$$\frac{I_p(\lambda_{ij})}{I_p(\lambda_{kl})} = \frac{N_i A_{ij}\, T(\lambda_{ij})\eta(\lambda_{ij})}{N_k A_{kl}\, T(\lambda_{kl})\eta(\lambda_{kl})} = \frac{1}{F_R}\frac{N_i A_{ij}}{N_k A_{kl}} \tag{2.3}$$

where$textitT_(\lambda)$ and $\eta(\lambda)$ are dependent on the spectrometer that is used for measuring the radiation. Here, the values were read from the data provided by the maker of the instrument. The Helium-I line intensity ratio in the above equation can be used to find electron temperature and density. The Helium Grotrian diagram in fig.[] shows the various Helium I transitions that were considered in order to measure electron density and temperature of the cold component of electron. A careful selection of a pair of lines is made such that the ratio of their intensities is either a strong

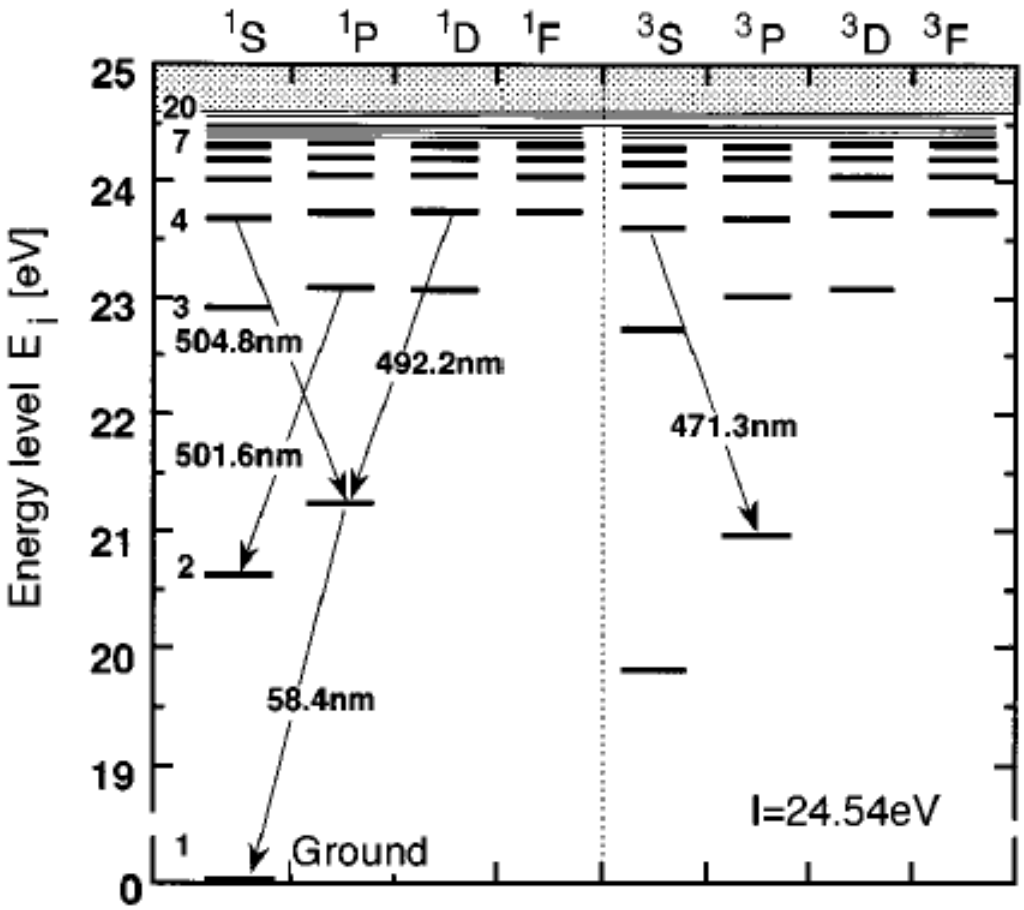

Figure 2.1: Partial helium Grotrian diagram showing various neutral Helium transitions.I is the ionization energy.Figure 1 of [6]

function of electron temperature or electron density.Once such ratios are found, they can be used to find electron temperature and density of the cold component in RT-1 plasma. For the aforementioned purpose, we calculated the various helium I line intensity ratios to determine which ratios are applicable in the density range of RT-1 plasmas. To that end, we calculated $492.2nm(4^1D \rightarrow 2^1P)/471.3nm(4^3S \rightarrow 2^3P$, $501.6nm(3^1P \rightarrow 2^1S)/471.3nm(4^3S \rightarrow 2^3P)$, $504.8nm(4^1S \rightarrow 2^1P)/471.3nm(4^3S \rightarrow 2^3P)$, $501.6nm(3^1P \rightarrow 2^1S)/492.2nm(4^1D \rightarrow 2^1P)$ and $728.1nm(3^1S \rightarrow 2^1P)/706.5nm(3^3S \rightarrow 2^3P)$HE-I line intensity ratio databases- with respect to temperature and density- from ADAS database to estimate the electron temperature. For density estimation of the cold component of electrons, we calculated the$492.2nm(4^1D \rightarrow 2^1P)/504.8nm(4^1S2^1P)$, $501.6nm(3^1P \rightarrow 2^1S)/504.8nm(4^1S \rightarrow 2^1P)$, $501.6nm(3^1P \rightarrow 2^1S)/492.2nm(4^1D \rightarrow 2^1P)$and $667.8nm(3^1D \rightarrow 2^1P)/728.1nm(3^1S \rightarrow 2^1P)$ He I line intensity ratio databases from the ADAS database.

The helium line intensity ratio databases mentioned above were calculated from the population densities of the excited levels from where these line intensities originate. The population densities of the related excited levels were brought from the ADAS atomic database[15], access to which was provided by the National Institute of fusion Sciences (NIFS).

Out of the aforementioned Helium I line intensity ratio databases,$501.6nm(3^1P \rightarrow 2^1S)/471.3nm(4^3S \rightarrow 2^3P)$ and $728.1nm(3^1S \rightarrow 2^1P)/706.5nm(3^3S \rightarrow 2^3P)$ were found

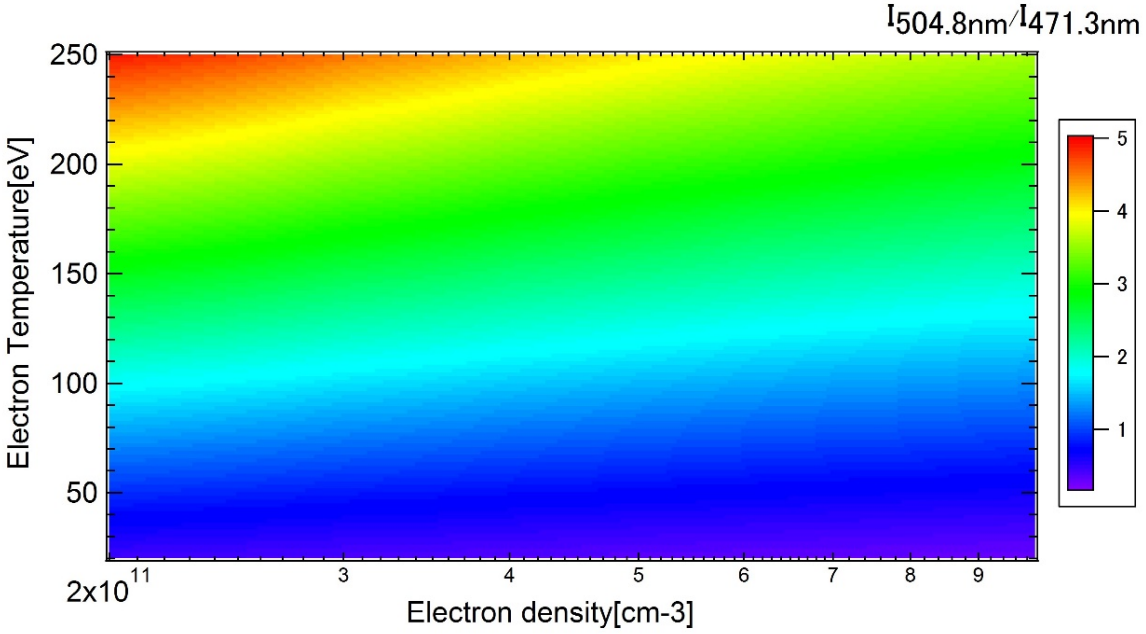

Figure 2.2: Database showing $I_{504.8nm}/I_{471.3nm}$w.r.t to electron density and temperature

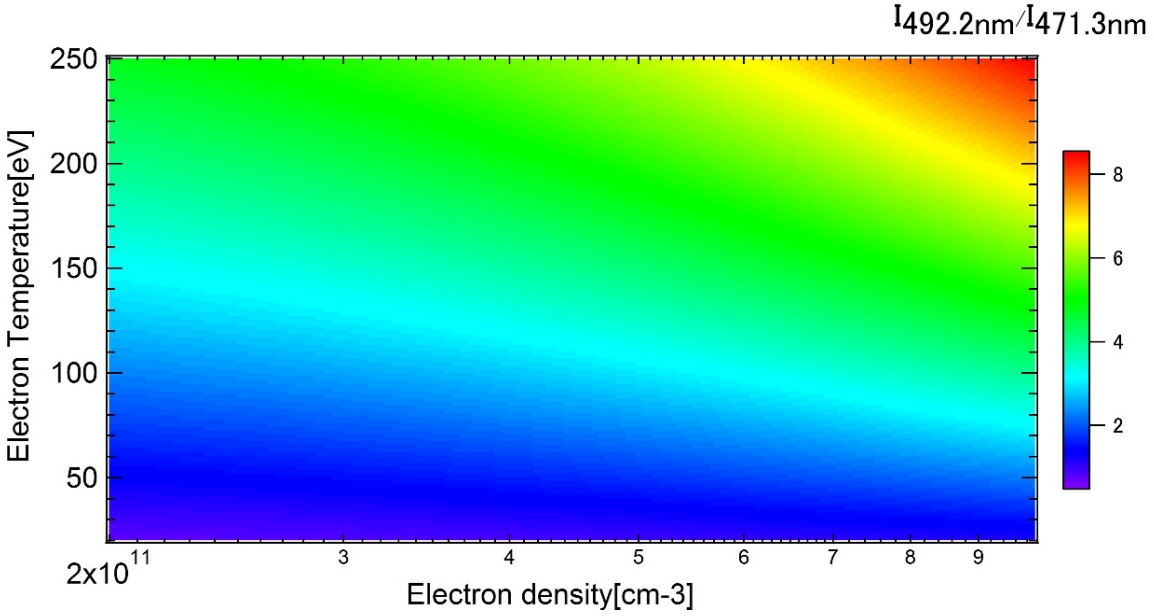

Figure 2.3: Database showing $I_{492.2nm}/I_{471.3nm}$w.r.t to electron density and temperature

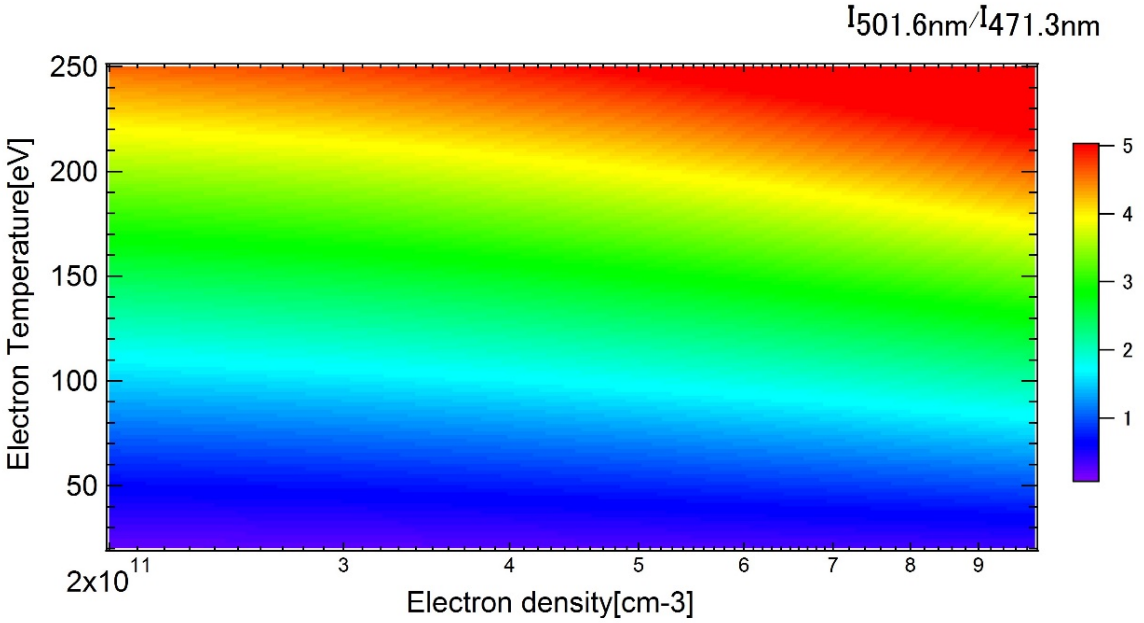

Figure 2.4: Database showing $I_{501.6nm}/I_{471.3nm}$w.r.t to electron density and temperature

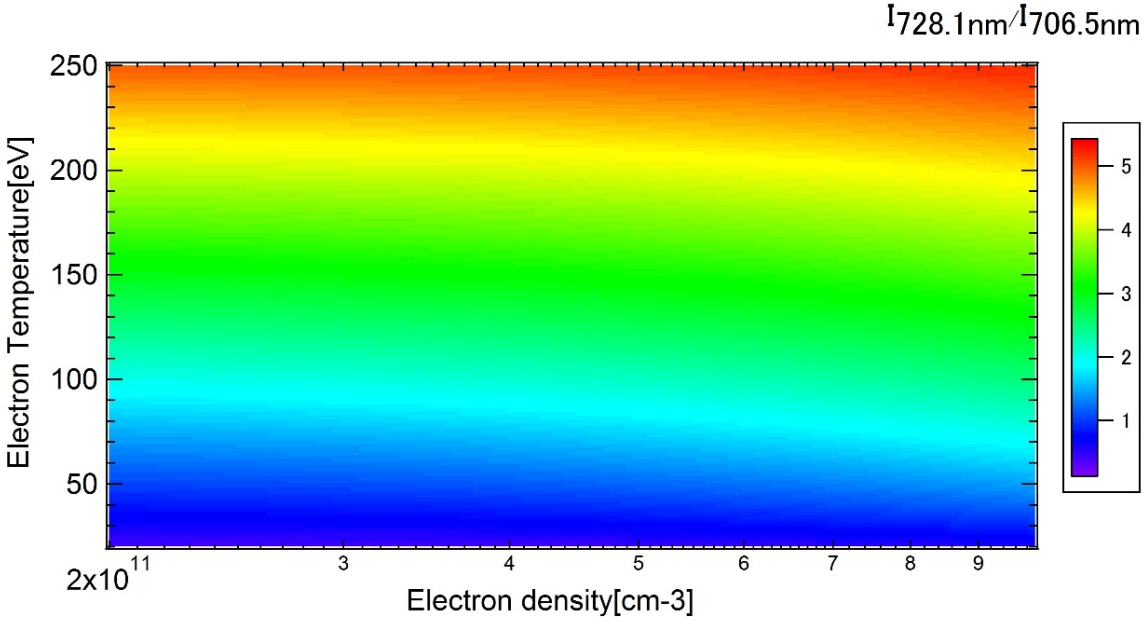

Figure 2.5: Database showing $I_{728.1nm}/I_{706.5nm}$w.r.t to electron density and temperature

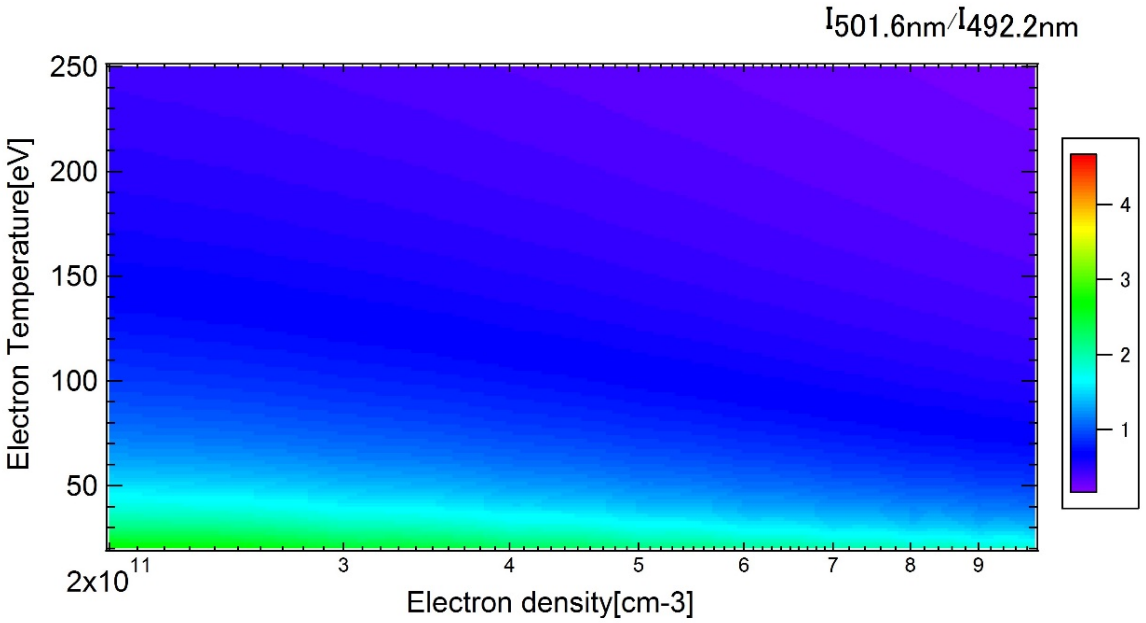

Figure 2.6: Database showing $I_{501.6nm}/I_{492.2nm}$w.r.t to electron density and temperature

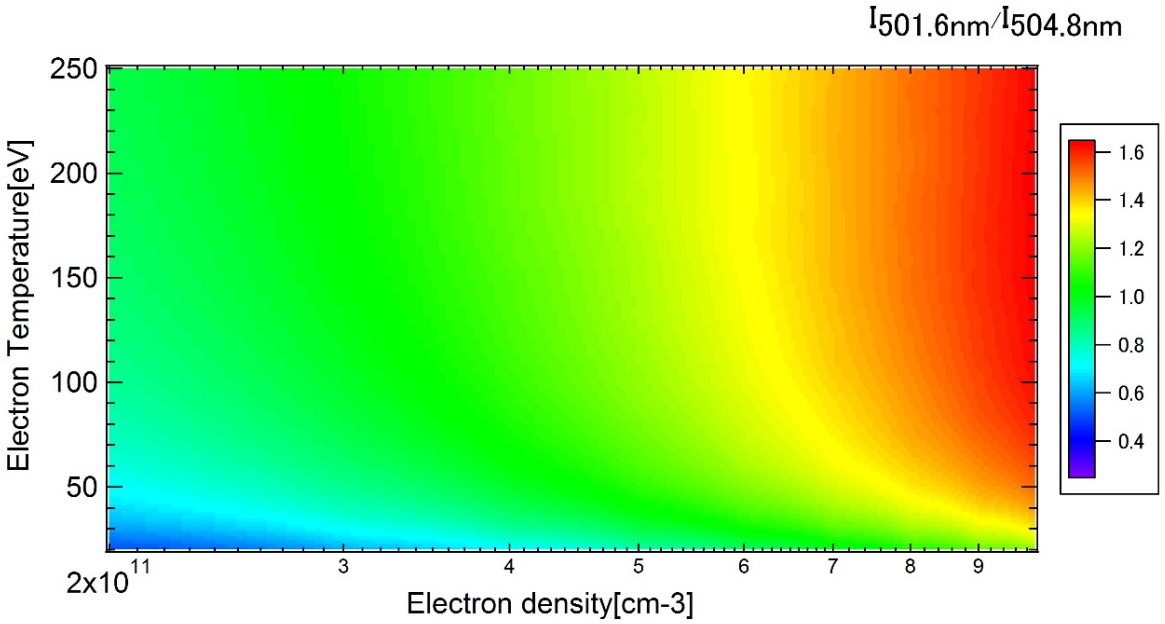

Figure 2.7: Database showing $I_{501.6nm}/I_{504.8nm}$w.r.t to electron density and temperature

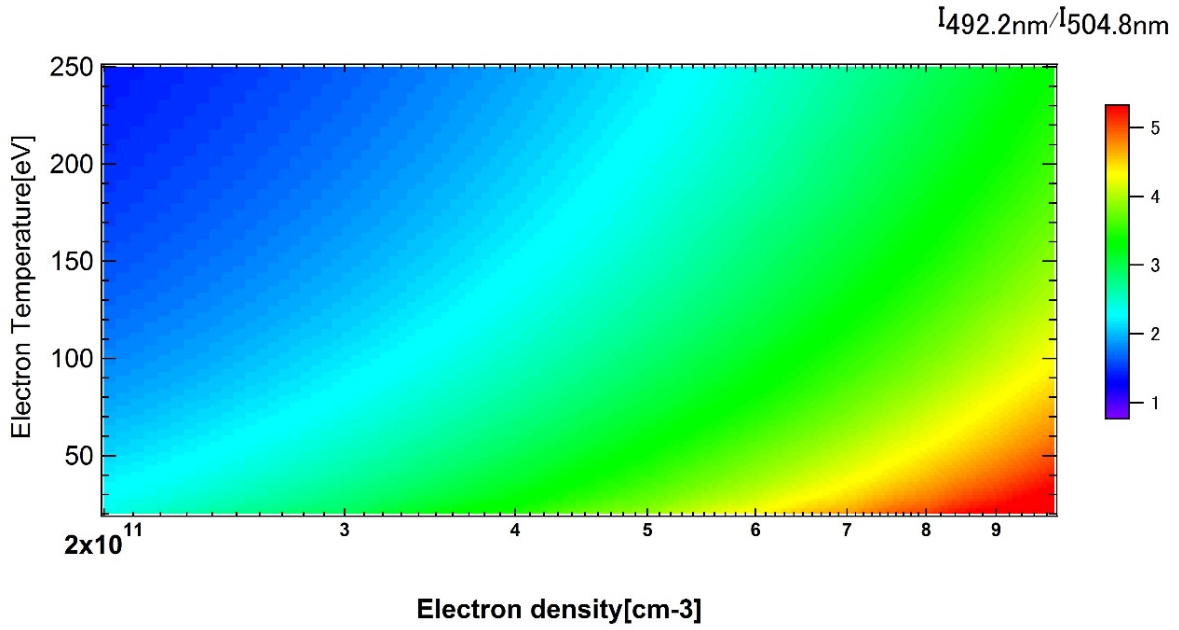

Figure 2.8: Database showing $I_{492.2nm}/I_{504.8nm}$w.r.t to electron density and temperature

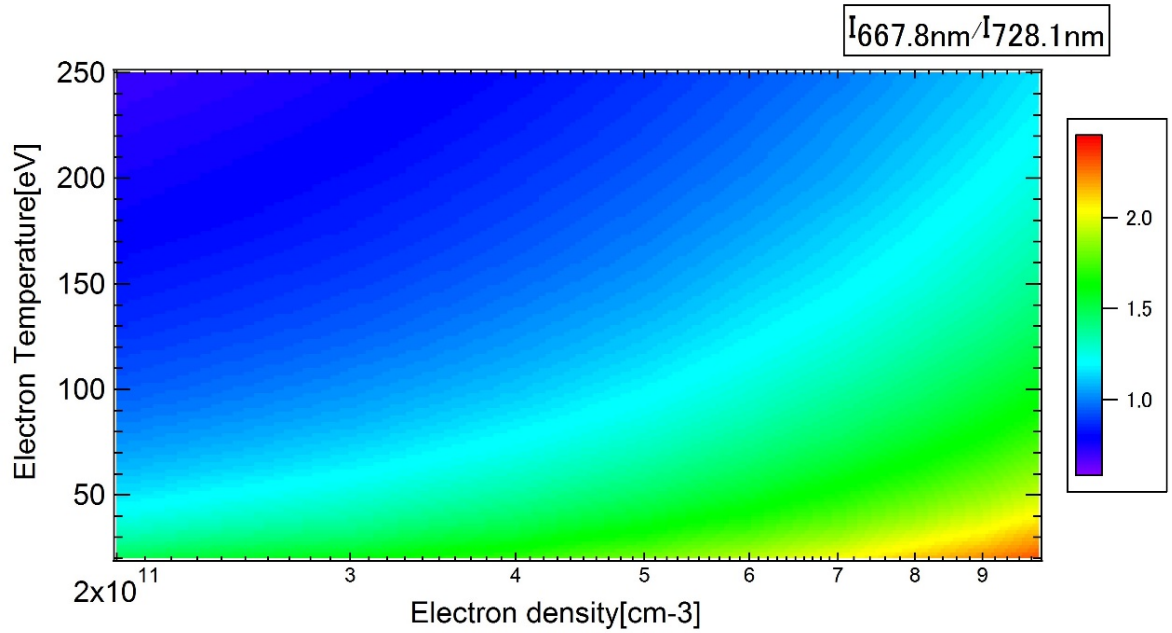

Figure 2.9: Database showing $I_{667.8nm}/I_{728.1nm}$w.r.t to electron density and temperature

to be more dependent on the temperature and less dependent on the density in the density regime of RT-1, and therefore have been used to calculate the temperature of the cold component of the electron in this research. However,$492.2nm(4^1D \rightarrow 2^1P)/504.8nm(4^1S \rightarrow 2^1P)$ helium I line intensity ratio- as is evident from the figure[]- is a strong function of the electron density and weak function of the electron temperature in the density regime of the RT-1 plasma. Although, both $501.6nm(3^1P \rightarrow 2^1S)/471.3nm(4^3S \rightarrow 2^3P)$ and $728.1nm(3^1S \rightarrow 2^1P)/706.5nm(3^3S \rightarrow 2^3P)$ show a strong temperature dependence, in this research, we have given preference to $501.6nm(3^1P \rightarrow 2^1S)/471.3nm(4^3S \rightarrow 2^3P)$ ratio for the purpose of estimating the electron temperature of the cold component, for the following reasons. The spectral lines used to find the ratio can be taken simultaneously measured with the pair of lines used to estimate the density profile, in a single snapshot- that reduces the machine time required. Secondly, the transition energies for the lines 492.2 nm, 504.8 nm,471.3 nm and 501.6 nm-used here- are relatively much closer to each other than 706.5nm and 728.1nm ; thus, are naturally more suitable for the purpose of estimating the temperature and density profile than the latter pair. In order to confirm our observations, we compared the orthogonality between the various ratios used here for estimation of the density and temperature. The results are shown in the following graphs. The color red is equal to 1 whereas the color blue is equal to 0. Therefore, blue regions on the graph represent areas where a pair of ratios is more orthogonal and more suitable to be utilized for estimating the density and temperature profile.

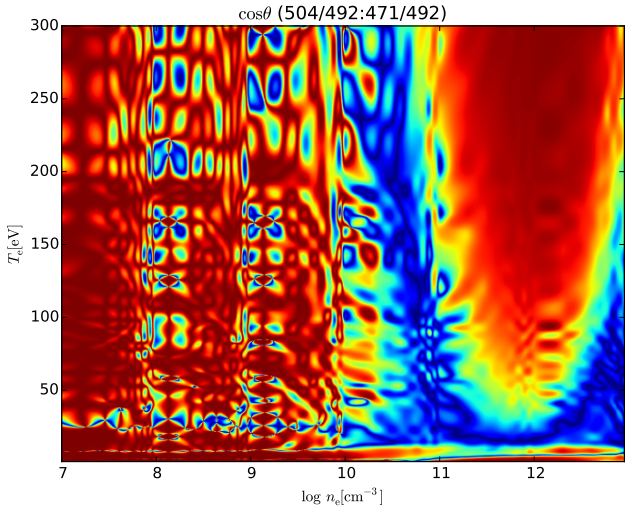

Figure 2.10: Orthogonality between the ratios 471.3nm/492.2nm and 492.2 nm/504.8nm. Figure provided by Y.Kawazura

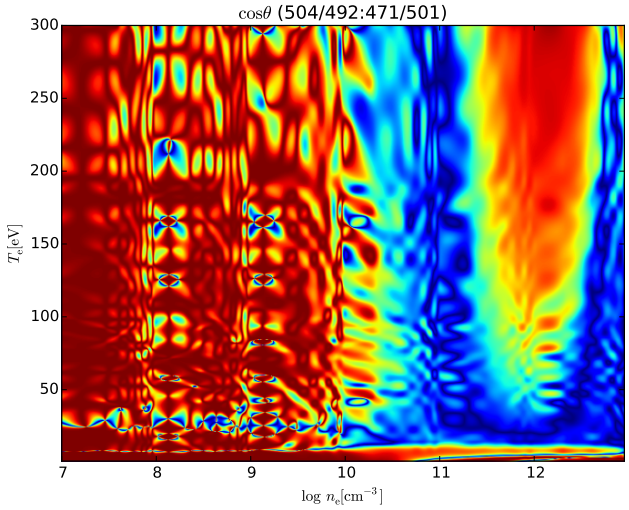

Figure 2.11: Orthogonality between the ratios 501.6 nm/471.3 nm and 492.2 nm/504.8nm.Figure provided by Y.Kawazura

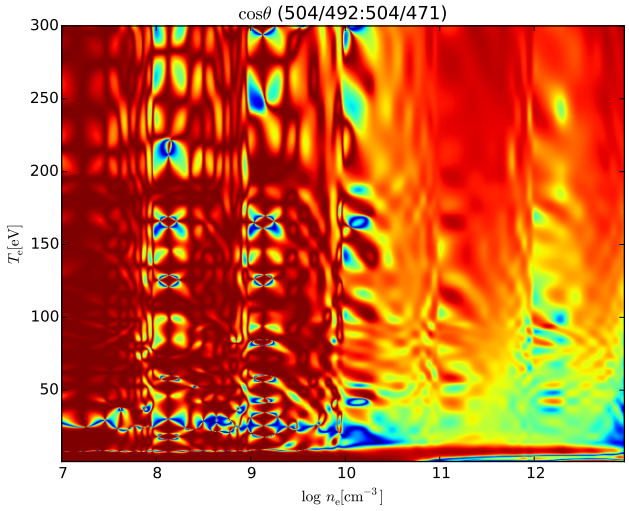

Figure 2.12: Orthogonality between the ratios 504.8 nm/471.3 nm and 492.2 nm/504.8nm.Figure provided by Y.Kawazura

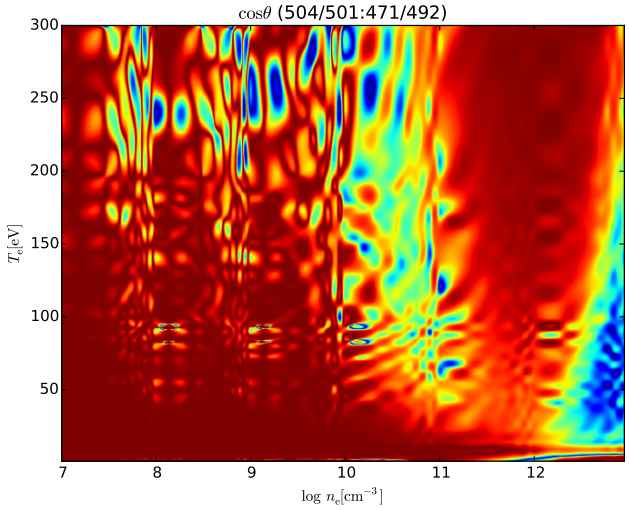

Figure 2.13: Orthogonality between the ratios 492.2 nm/471.3 nm and 501.6 nm/504.8nm.Figure provided by Y.Kawazura

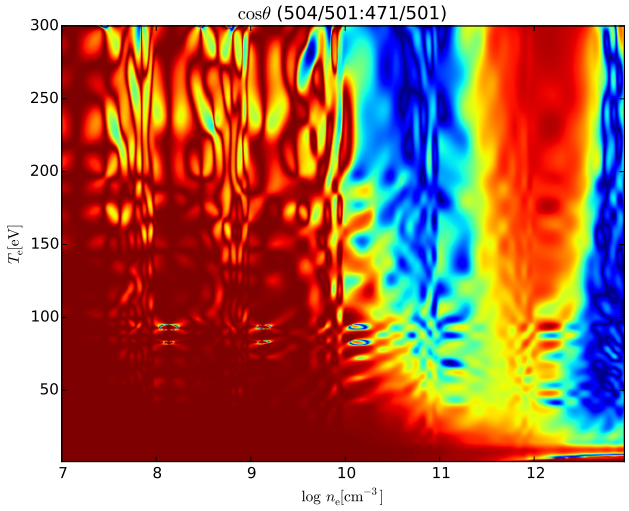

Figure 2.14: Orthogonality between the ratios 471.3nm/501.6 nm and 501.6 nm/504.8nm.Figure provided by Y.Kawazura

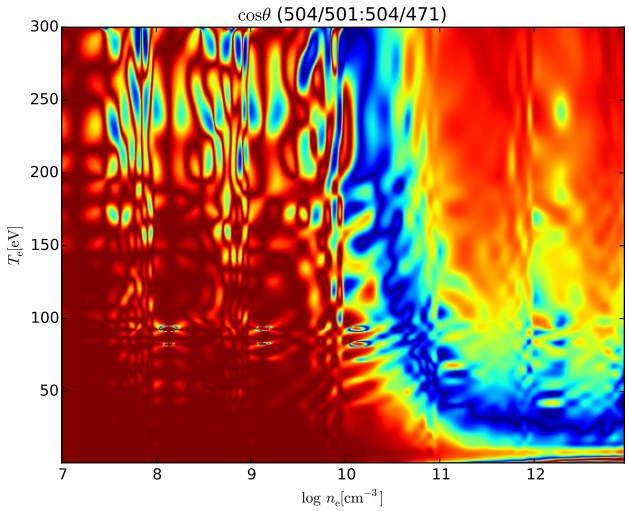

Figure 2.15: Orthogonality between the ratios 501.6 nm/504.8 nm and 471.3 nm/504.8 nm.Figure provided by Y.Kawazura

As can be seen from figure 2.11, orthogonality is best between 501.6 nm/471.3 nm and

492.2 nm/504.8 nm helium line intensity ratios- in the density regime of RT-1.Thus in this research, we have employed the above mentioned helium line intensity ratios to find the density profile of the cold component of electron.Moreover,the ratios used here have successfully been used to estimate electron density and temperature in the past[6].

2.2 Collisional Radiative model

The population densities of the various excited energy levels of neutral helium have successfully been calculated by the application of the following two models- Steady State Corona model (SSC) and Collisional Radiative model. The steady state corona model can be used to find the population densities of the excited level of an atom, provided it satisfies the criterion for the applicability of the method. For the steady state corona model to be applicable to a certain atom, it must satisfy the following conditions: the electron velocity distribution can be described by Maxwellian distribution, the ion temperature must be less than or equal to the electron temperature, and the plasma should be optically thin to its own radiation. The presence of hot electrons causes the electron velocity distribution to deviate from the Maxwellian velocity distribution. However, in case of RT-1 plasmas hot electrons, due to their extremely high energies- around 10KeV, do not interact either with the ions or the cold component of electrons. Therefore, the electron temperature calculated through this method solely represents the cold component of the electrons, and contains only a negligible percentage of hot electron component. The Steady state corona

model assumes that all the line emissions are the result of a single collision between the electrons and the atoms in the ground state, followed by a direct radiative de-excitation. The secondary state corona model can predict the population densities of the excited levels of a certain atom with considerable accuracy for electron densities [$n_e < 10^{11} cm^{-3}$. However, for electron densities higher than$10^{11} cm^{-3}$, other secondary processes such as excitations from neighbouring levels and excitation from metastable states becomes dominant, and a different model must be thought in order to find the population densities of the excited levels accurately. As mentioned above, at higher electron densities the simple assumptions of secondary state corona model are no longer valid, since secondary processes involving collisions with the excited levels and ionized atoms become increasingly dominant, and must be taken into consideration for calculating the population density of various excited levels. Some of the important secondary processes are volume recombination-recombination collisions contribute to the emitting level population, collisions between the ground state atoms and the excited state atoms- this results in the highly excited atom losing a part of its energy to the atom in the ground state which further results in the formation of one or more excited atoms, cascading redistribution affects(this involves the electron impact excitation of a highly excited level and then transition to an upper energy level), excitation transfer collisions(the upper energy levels are either depopulated or populated by the excited transfer collisions), and excitation from metastable collisions(the upper energy levels get excited by collisions with electrons and metastable energy

levels). The cold component of electron of the plasma-created during the experiments-is considered to be of moderate densities$n_e < 10^{12}cm-3$ and low temperature(¡200eV). One of the reasons for such an assumption is that the cut-off density of Electron cyclotron heating for RT-1 plasmas is less than $10^{12}cm-3$. In such regimes of temperature and densities, many of the secondary processes can be neglected. The recombination rates at the aforementioned densities is much smaller than the excitation rates, and therefore the effects of volume recombination can be considered to be negligible[17]. The cascading redistribution effects are only important if the electron temperature is comparable to the upper energy levels; however, in case of helium, the first excited level (n=1) is 19.8eV[51], and therefore, the redistribution effects of the higher energy levels(n¿2) can be neglected. The collisions from the excitation transfer only get dominant if the energy of the upper line levels is comparable to the neighbouring levels. Furthermore, excitation transfer cross-sections are also larger when transitions are optically allowed.The contributions from the metastable states are important if the metastable states are closer to the ground state or if they are energetically closer to the emitting excited level. The collisional radiative model has been successfully used to calculate the population of the metastable states to great accuracy, and contributions from the metastable states ha successfully been incorporated in calculating the population densities of the excited energy levels. Unlike steady state corona model, the collisional radiative model assumes that the bound excited level populations are not exclusively from the ground state due to electron impact excitation.

In this model, the contribution from all the secondary processes like excitation transfer, recombination and ionization involving all the excited levels is incorporated. The criterion for the applicability of the collisional radiative model is as follows[24]:the electron velocity distribution can be described by a Maxwellian, the ionization process is by electron collision from any bound level and is partially balanced by three body recombination into any level, excitation transfer between any two bound levels is by electron collisions, radiation is emitted when a bound electron makes spontaneous transition to a lower level or when a free electron makes a collision-less transition to a bound level,and that the plasma is optically thin particularly to its own radiation. An equation based on collisional radiative model describing the population density $N_i$of the respective level can thus be written as follows:

$$\frac{dN_i}{dt} = n_e \sum_{j \neq i} S_{ji} N_j + \sum_{j>i} A_{ji} N_j - n_e \sum_{j \neq i} S_{ij} N_i - \sum_{j<i} A_{ij} Ni - n_e I_i N_i = 0 \qquad (2.4)$$

The terms $I_i$the ionization rate coefficientsand $S_{ji}$the excitation and de-excitation rate coefficients, in the above equations re all functions of electron temperature and electron density. The first term in equation(1) corresponds to excitation or de-excitation of the electron population of levels j that end up at level i. The second term represents the spontaneous de-excitationallowed transitions from higher levels j to i. The third term corresponds the de-excitation of level i and the fourth term corresponds to the allowed spontaneous de-excitations originating from level i. The final term in the equation is

associated with the ionization rate of the electron population of level i. Equations similar to the one above can be written for each level of a neutral helium atom, and thus we have N(level number) coupled differential equations. Solving these N(level number) coupled differential equations simultaneously provides us with the population density of the energy level from where the line originates. The procedure is repeated one more time for the second transition. Once the population densities of the energy levels,from which the lines emit, are known, the population densities can be used to find the required Helium line intensity ratios. The terms A_{ij} is very well known for all the transitions; however, other terms(S_{ij} are not very well known, and their calculation is quite complex.However in this research, we have used ADAS,an online atomic database system, that calculates the population densities- based on collisional radiative model- of energy levels from where the respective transitions originate.

2.3 Abel Transform

In the previous section, we have written Intensity I_p of a spectral line as a function of the population density N_i of the energy level i from where the spectral line originates.

$$I_p(\lambda_{ij}) = (4\Pi)^{-1} N_i A_{ij} V\Omega T(\lambda_{ij})\eta(\lambda_{ij}) \tag{2.5}$$

However, the Intensity of a spectral line, as measured by a CCD camera, is not the intensity emanating from a single point, but the line integrated intensity over the line of observation, as seen by the CCD camera. From the equation above, the line integrated intensity I_{line_Int} of a spectral line emitting from level i, over a line of observation L, can be written as follows:

$$I_{Line\_Int} = (4\Pi)^{-1} N_{i_{Line\_Int}} A_{ij}\, V\Omega\, T(\lambda_{ij})\eta(\lambda_{ij}) \tag{2.6}$$

We know that the population density N of an excited level is a function of electron temperature and electron density.The line integrated population density $N_{i_{Line\_Int}}$ of an emitting excited level i-along a line of measurement L-can therefore be written as:

$$N_{i_{Line\_Int}} = \int_L N_i(n_e(r_i, z_i), T(r_i, z_i))dl \tag{2.7}$$

where $n_e(r_i, z_i)$ and $T(r_i, z_i)$ are the electron density and the electron temperature of the cold component of electron at point (r_i, z_i) inside RT-1 plasma. Theoretically, if the density and temperature profile of electron inside RT-1 is known, it can be availed to calculate the line integrated intensity of the necessary spectral lines along a certain line of measurement, from which the line integrated intensity ratios can be found. Here, we have employed the inverse approach of calculating the density and temperature profile from a pair of helium line intensity ratios, measured experimentally. The temperature and

density of the cold component of electron are assumed to be functions of magnetic flux surface/psi and the ratio of the magnetic field strength along/$psi$and the magnetic field ratio at the equator along the sameψ, $B_\psi/B_{\psi,z=0}$, as shown by the following equations.

$$T_e(r,z) = T_e(\psi(r,z), B_\psi/B_{\psi,z=0}(r,z)) \tag{2.8}$$

$$n_e(r,z) = n_e(\psi(r,z), B_\psi/B_{\psi,z=0}(r,z)) \tag{2.9}$$

The figures below show the poloidal cross-section of the magnetic flux surfaceψ and magnetic ratio$B_\psi/B_{\psi,z=0}$ inside RT-1, for both the scenarios of levitation and non-levitation.

The information about the magnetic fluxψ and the magnetic ratio $B_\psi/B_{\psi,z=0}$ inside

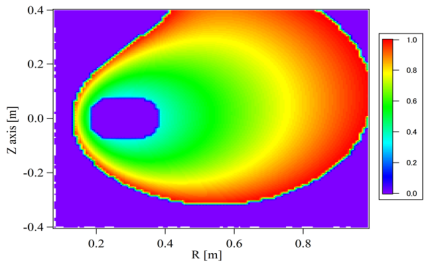

(a) magnetic flux insideψ inside RT-1 during levitation

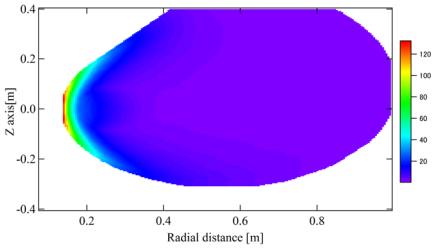

(b) $B_\psi/B_{\psi,z=0}$ inside RT-1 during levitation

Figure 2.16: ψ and $B_\psi/B_{\psi,z=0}$ during levitation

RT-1 have been used in concert with the experimental measured line intensity ratios to find the density and temperature profile of the cold component of electron inside RT-1 plasma. Firstly, suitable functions for electron temperature and density in terms of/psi and $B_\psi/B_{\psi,z=0}$ are thought. Then, for a suitable set of function parameters, an appropriate initial value of the density profile is calculated. Using the initial value for the

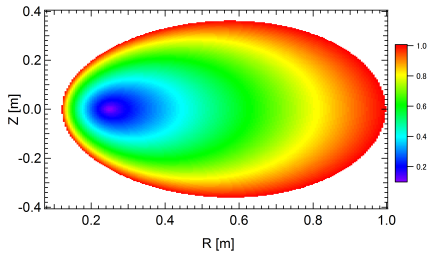

(a) magnetic flux insideψ inside RT-1 during support

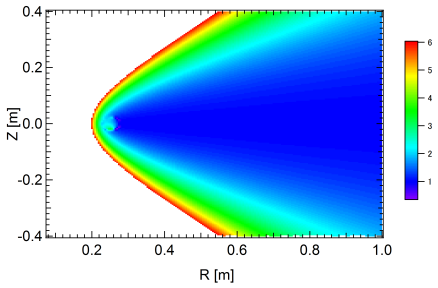

(b) $B_\psi/B_{\psi,z=0}$ inside RT-1 during support

Figure 2.17: ψ and $B_\psi/B_{\psi,z=0}$ during support

density profile, and the function for the temperature, fitting is performed to the experimentally measured temperature sensitive line intensity ratios, and a temperature profile of the cold component of electron. Then, using the obtained temperature profile and the density function, fitting is performed to the experimentally measured density- sensitive line intensity ratios to obtain a density profile. The obtained profile is used to find the temperature profile again, and the process is repeated until a self-consistent solution is obtained for electron temperature and density. In simple terms, the process is repeated until the temperature profile- obtained from the density profile- gives back the original density profile-before any fitting is performed. The figure 2.11 explains the process of convergence to a self-consistent in a simplistic manner.

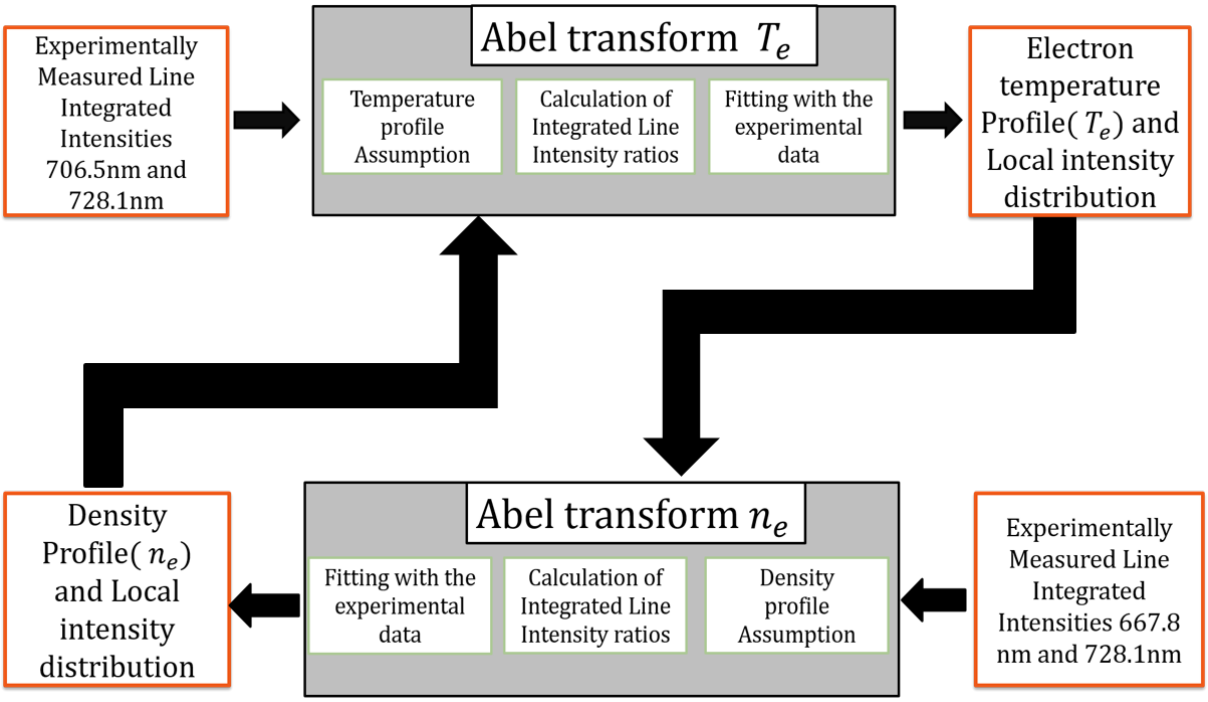

Figure 2.18: Flowchart showing the process of Abel transform used in this research simplistically

Chapter 3

Experimental setup

3.1 Ring Trap 1, the artificial magnetosphere

Ring Trap, RT-1, is the artificial laboratory magnetosphere that confines ultra-highβ plasma in a dipole magnetic configuration, which is generated by levitating a superconducting coil. Figure 3.1 shows the superconducting coil made of high temperature superconducting Bi-2223 wires, which generates a dipole magnetic field. By operating the the superconducting coil in RT-1 is operated in a permanent current mode and magnetically levitating the coil with the help of a feedback controlled normal conducting electromagnet- situated at the top of RT-1(figure 3.2)- turbulence in the plasma is substantially minimized. During levitation, laser sensors are used to detect the height of the levitated coil, and in response to any sudden vibrations of the coil, the current in the levitating coil is adjusted accordingly- via feedback-to maintain the stability of the levitating coil. The su-

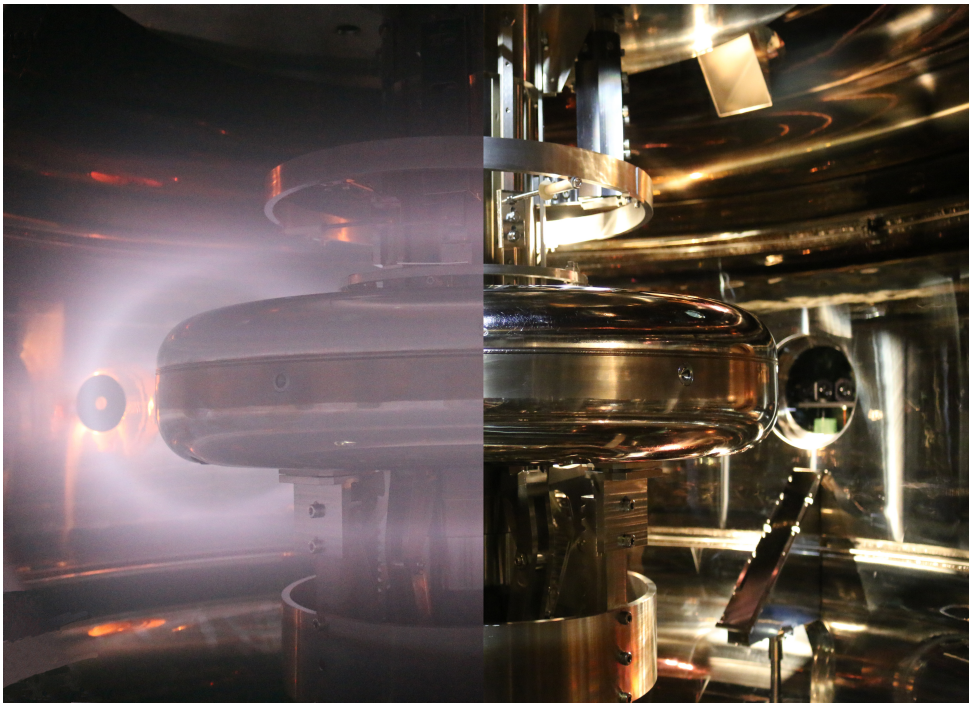

Figure 3.1: Figure showing the superconducting coil used to create dipole magnetic configuration inside RT-1 which confines the high beta plasma. Figure of [7]

perconducting and levitation coils in RT-1 are operated at 250 and 28.8 kA, respectively. The combination of the two magnets gives rise to separatrix configuration, as can seen in figure 3.3. However, when the coil is not levitated and supported on a metal stand, the configuration is the basic dipole configuration. The superconducting coil is cooled down to 20K using 3 GM refrigerators, and the experiments are usually conducted for 6 hours, after which the temperature of the coil rises to 30K. As can be seen in figure 3.2, a system of new correction coils were placed around RT-1 to cancel out the geomagnetic field and prevent the tilting of the floating coil. For the current operations,the plasma is created by Electron Cyclotron Resonance Heating microwaves of 25kW at 8.2GHz (1s) and 20kW(2s)

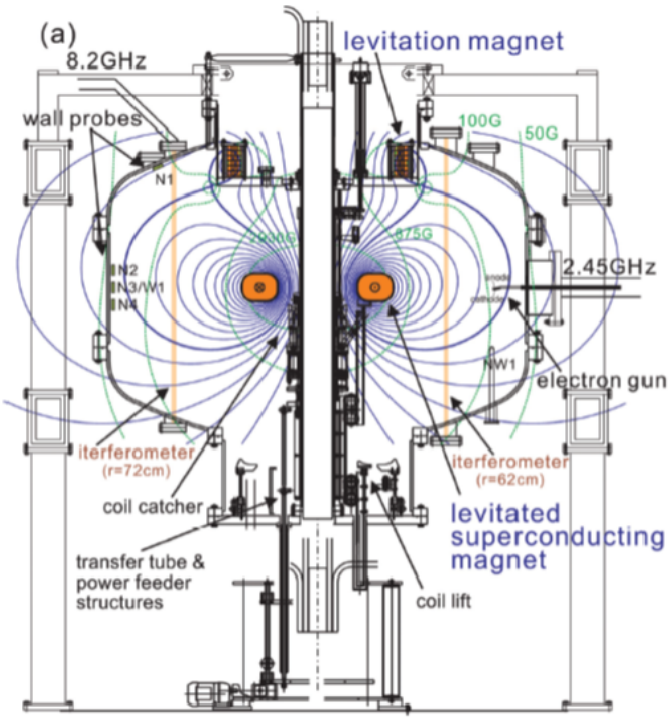

Figure 3.2: Cross-section view of RT-1 showing all the essential equipments used.Figure of [8]

at 2.45GHz. The gases typically used for experiments are helium and hydrogen; however, recently experiments involving argon gas have also been successfully carried out. Figure 3.4 shows the parameter specification of the main components of RT-1.

3.2 Diagnostic and measurement systems in RT-1

There are many essential quantities such as magnetic field, electric field and line integrated intensity,x-ray emission that must be measured. For the above mentioned purpose, the following devices have been placed on RT-1: Dia-magnetic loop, photo-diode,

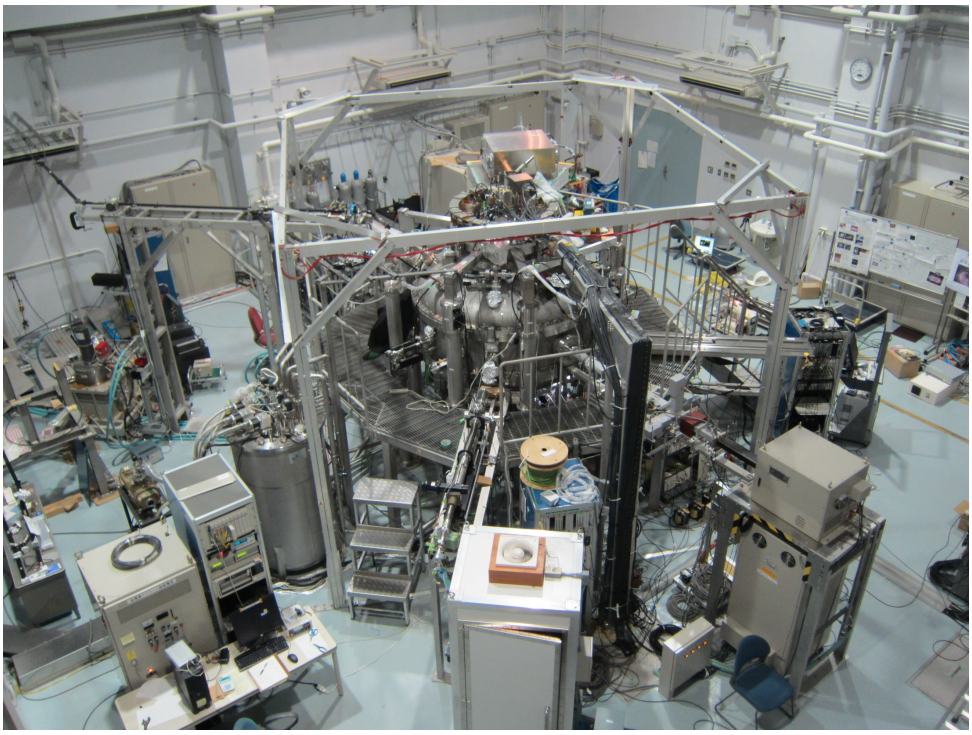

Figure 3.3: Photograph showing the top view of RT-1 device. Figure of [9]

X-ray camera, video camera, soft x-ray measurement device, electron interferometry,Q mass,Double probe,ion probe, Langmuir probe, thermal probe,Hall device probe, near ultra-violet and visible range spectrometer, pockels device. The diagnostic and measurement systems used in this research are as follows:

•Dia-magnetic loop: Inside RT-1, the upper part of the levitating coil, coil surface and the outer surface of the vacuum vessel below the coil is wrapped with dia-magnetic loop that measures the diamagnetic signal when the plasma is created and calculates the pressure profile of plasma in RT-1 through a pair of equilibrium chords.

•Video camera: By viewing the plasma discharge through a video camera, one can

Superconducting Coil	
Coil dimensions	W=193mm,H=150mm
Superconducting material	Bi-2223
No. of Turns	2160
Specified current	116A
Specified magnetic power	250kA
Magnetic field strength	100~1000G
Super Conducting Temperatures	20K~30K

Refrigerating Machine	
Maximum specified cooling capacity	60W(at20K)
Maximum gas capacity	2g/sec
Cooling time(Room temp.→20K)	45 hours

Levitating coil power source	
Specified Current	1,300 A
Controlling Current	±150A(20Hz)
Controlling method	Switching Regulator
Cut Off speed	100 ms

Vacuum Vessel	
Dimensions	R=1000mm,Z=560mm
Volume	$3.7m^3$
Achieved Vacuum	$7\times 10^{-6}Pa$
Total weight	3 ton

RF ECRH 1	
Transmission frequency	8.2GHz
Maximum standard power	100kW,1sec
Generation tube	Klystron

RF ECRH 2	
Transmission frequency	2.45GHz
Maximum standard power	20kW
Generation tube	Magnetron

Levitating coil	
Coil dimensions	W126mm,H=157mm
Self inductance	4.6mH
Resistance	26mΩ
No. of Turns	68 turns
Maximum specified current	1,300A
Maximum specified Magnetic power	88kA
Weight	600kg

Pure water cooling system	
Specified heat extraction capacity	383kW
Maximum capacity	1000L/min

Figure 3.4: Tables showing the specifications of various components inside RT-1

monitor the plasma without getting showered by injurious X-rays and microwaves.

•Electron interferometry: The total electron density RT-1 plasma is measured with the help of a set of 3 interferometers. Two of them are placed vertically at a distance of 630 mm and 720 mm from the central axis of RT-1 and one horizontally at a distance of 450 mm from the central axis of RT-1. By measuring the line integrated electron densities through a set of 3 interferometers, one can interpolate the electron density profile(hot component + cold component) inside RT-1 by using a suitable fitting function.

•Qmass: Qmass measures the ratios of the various gases inside RT-1. It is used to monitor the amounts of the impurities and the mixture of 2 distinct gases. However, Qmass can not be used during the plasma shot or if the plasma pressure is above 5 mPa.

•Probe diagnostics: In RT-1, probe diagnostics has been used very effectively to measure quantities such as electron temperature, ion temperature and electron density. However, as the temperature of the hot component of electron inside the central region is extremely high, the probe measurements can only be used to investigate the periphery of the plasma inside RT-1.

•Spectroscopy: Spectroscopy is the method that has been utilized to find the temperature and density profile of the cold component of electron in this research.A detailed description of the spectroscopic set up is provided in the next section.

3.3 Spectroscopic System

Passive spectroscopy is an efficient method to measure various properties of plasma indirectly without any need to insert any probe for diagnostics. Spectrometer is a device, used in spectroscopy, that divides the incoming light into its constituent spectral lines and measure their wavelength and intensities. There are many kinds of spectrometers such as prism spectrometer, Fabry-Perot spectrometer,however the spectrometry generally used for observing radiation from plasma is Czerny-Turner configuration- with a planar reflecting grating. Figure 3.5 gives a simplistic schematic description of the Czerny-Turner configuration. The spectrometer used for measuring intensity emanating from plasma in

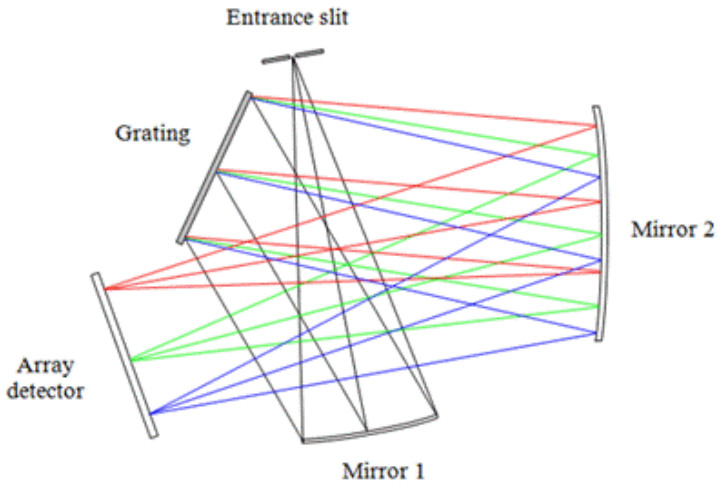

Figure 3.5: Simplistic working of Czerney-Turner configuration of spectroscopy. [10]

this research is SOL-II MS3504i spectrometer(0.35m) fitted with an ANDOR iDus 420 CCD(charged coupled device)as shown in figure 3.5. The detector of the spectrometer is

cooled in synchronicity with the measurement in order to suppress the noise in the measurement. After entering the slits of a spectrometer, the light hits the mirror collimator, then the grating, and after hitting the camera mirror it enters the CCD detector.

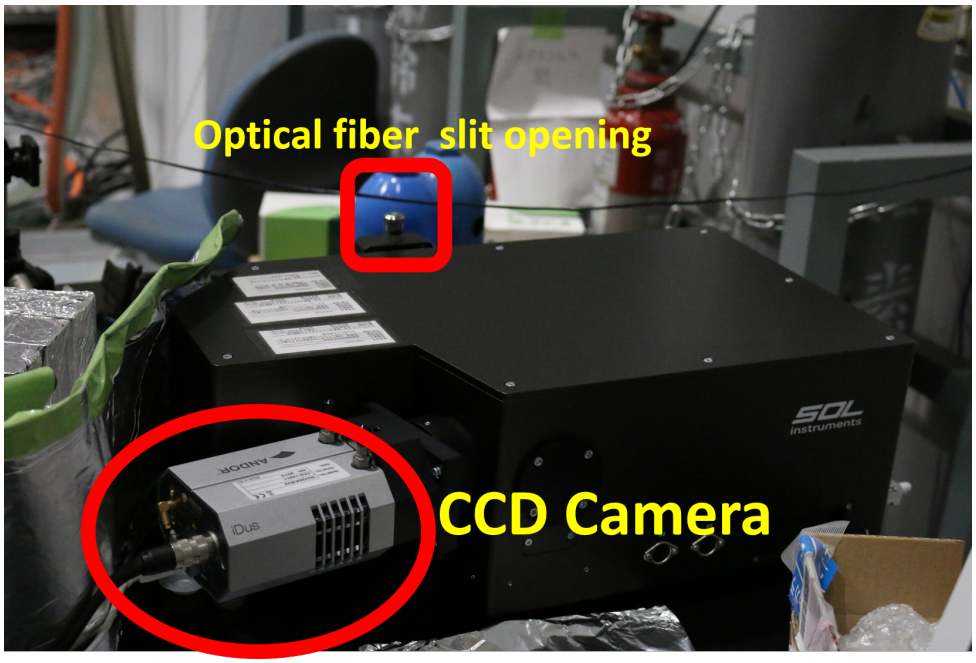

Figure 3.6: Image showing the MS3504i spectrometer used in the research

The size of a spectrometer corresponds to its resolution power and the light intensity it can take. The bigger dimensions of a spectrometer are greater is the resolution power of the spectrometer and more is the brightness of the spectral lines detected by the spectrometer. The length of a spectrometer used for this research is 0.35m.Because F(the quantity that expresses the brightness of a spectrometer) is relatively less, and as the grating and fibre corresponds to the near ultra-violet region, it is used to measure the weak signal of ions and determine their valency. Furthermore, as the grating of the used

spectrometer can be changed through a software to view a wide spectrum-near ultra-violet and visible region, it has been used in this research to detect and measure the helium I line intensities, and estimate the density and temperature profile of cold component of electrons.

Table 3.1: Table showing specifications for the SolarII MS3504i spectrometer

0.35 m Czerny-Turner Spectrometer	
F value	3.8
Wavelength resolution power	0.03/0.3
Reverse wavelength dispersion	1.19/11.9
Effective grating area[mm^2]	70×70
Number of Gratings per length[1/mm]	2400/300
Focal length [mm]	350
Observable Wavelength range[nm]	200-800

Table 3.2: Table showing specifications of the CCD camera attached to the spectrometer

Andor IDUS DU420A	
Number of pixels	1024× 255
Size of the element[μm]	26× 26
Observable Wavelength[nm]	200-800
Cooling temperature[C]	70×70

3.4 Experimental Setup

This section explains the experimental set up used to conduct experiments for this research. Measurements were mainly carried out through a collimator mounted on a rotating stage over an upper port of RT-1 as shown in figure 3.8. Also come measurements were made through a rotating collimator situated on a horizontal port of RT-1[fig. 3.9]. The

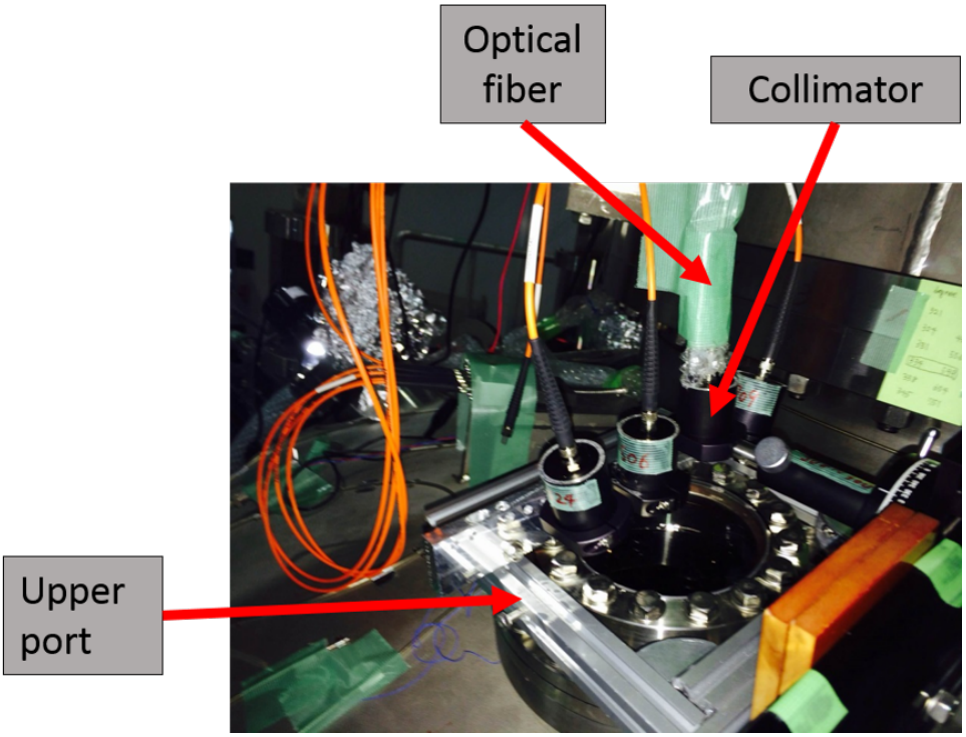

Figure 3.7: Experimental setup used for the vertical measurement from an upper port

radiation from the plasma confined in RT-1 is collected through the collimator, and passed through an optical fibre to the spectrometer, from where the signal is fed to a computer for further analysis. Figure 3.11 shows a schematic diagram of the whole process. As is understood from the figure, the experimental set up required to perform any spectroscopy

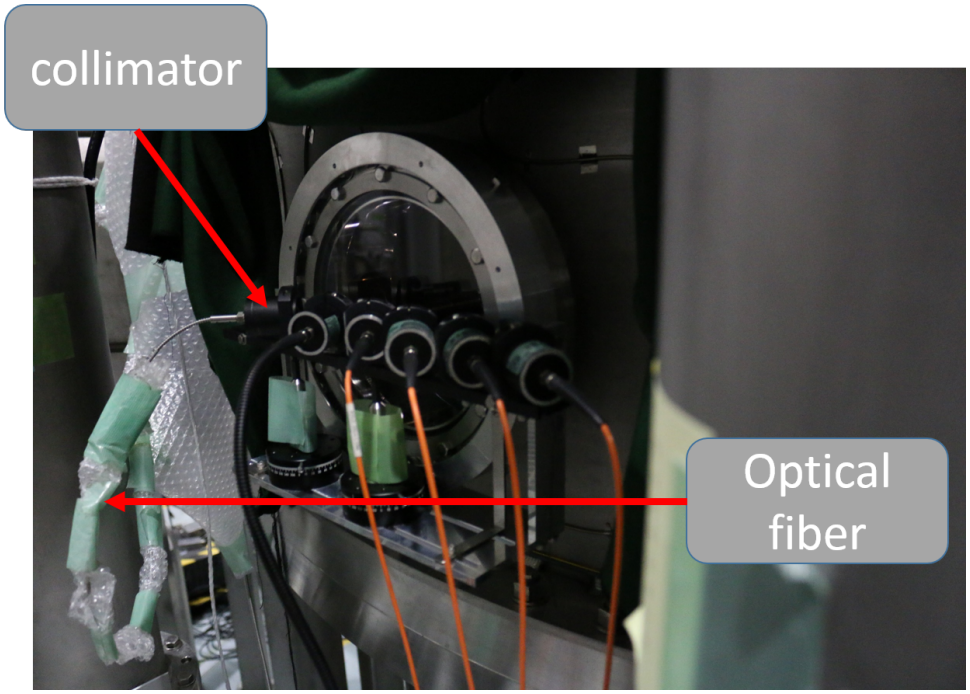

Figure 3.8: Experimental set up used for horizontal measurement from a horizontal port

is very simple and cost effective.By rotating the collimator-situated on an upper vertical port- we scan the line integrated helium I emissions coming from various regions of RT-1, and calculate the radial profile of the line integrated intensity ratios inside RT-1. Figure 3.10, briefly describes the experimental set up for the measurement from the upper vertical port.

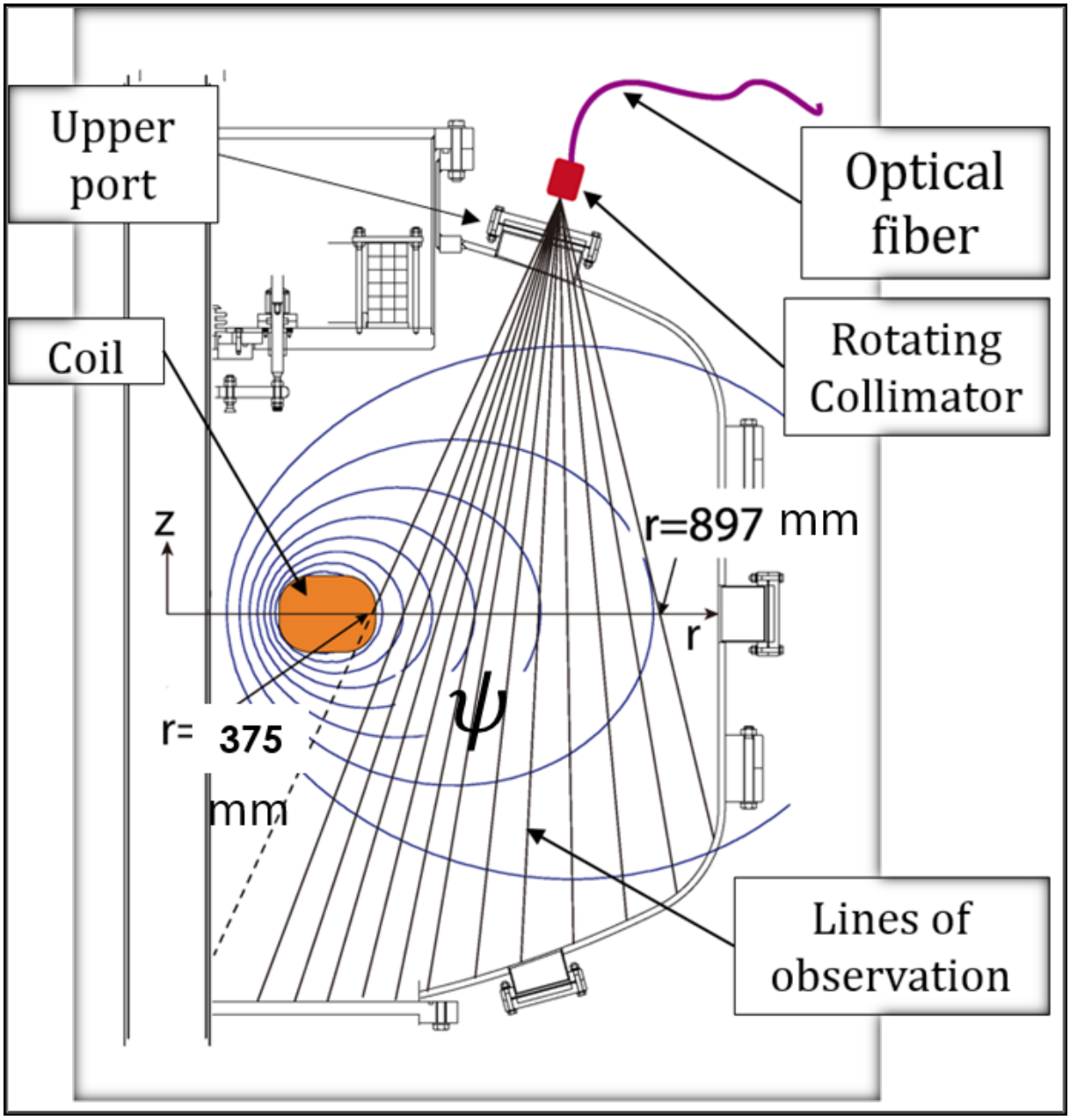

Figure 3.9: Schematic view showing the experimental procedure used to measure radial profile

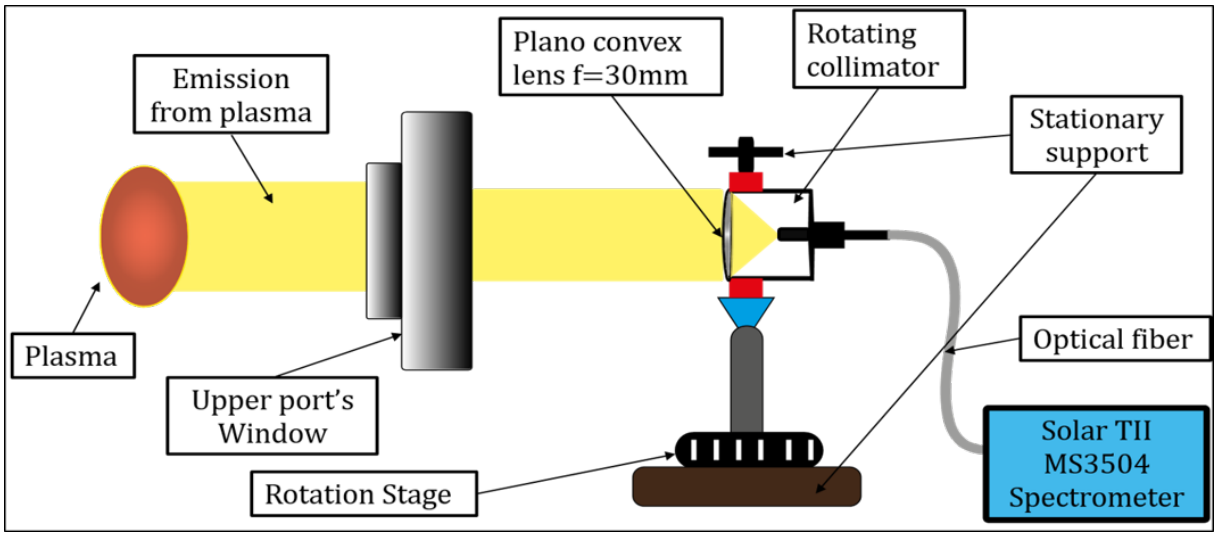

Figure 3.10: Schematic view of the emission emitting from plasma being collected by collimator

Chapter 4

Density and temperature profile

4.1 Data fitting

The intensities measured by the spectrometer are relayed to a computer for further analysis. Andor Solis- software used to control the MS3504i(0.35 m) spectrometer-receives the signals from the spectrometer and records the intensity along with the corresponding wavelength in a digital format. The digital data stored in the ASC format is then read by an IGOR macro. The respective spectral lines in the data are fitted with a gauss function and the area under the gauss is calculated which gives the total intensity associated with the spectral lines. Figure 4.1 gives a snap shot of the raw spectroscopic data.

The centre wavelength for the snapshot in the figure above is 470 nm. As can be seen in the above figure, various spectral lines in the raw spectroscopic data are overlapping onto each other. The problem was solved by using a package known as Multi-peak fitting

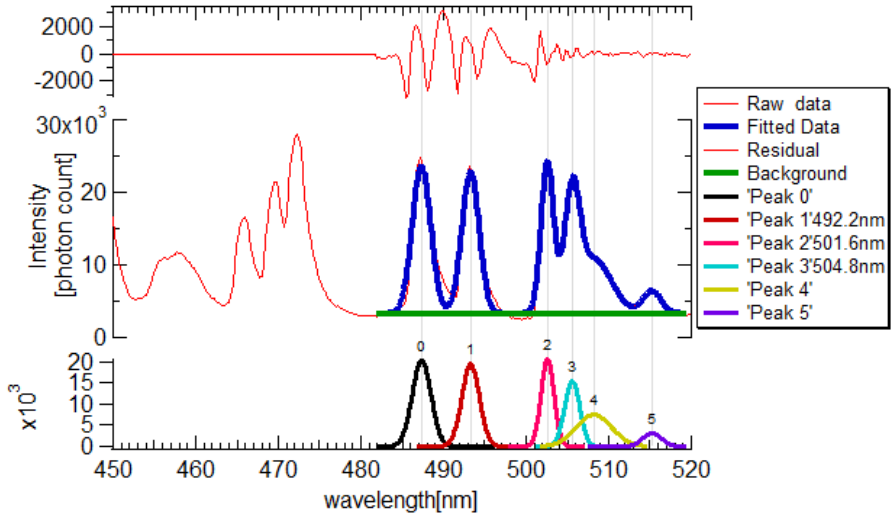

Figure 4.1: Figure showing the snap shot of the raw spectroscopic data and multi-peak fitting used to reconstruct 492.2 nm,501.6 nm and 504.8 nm

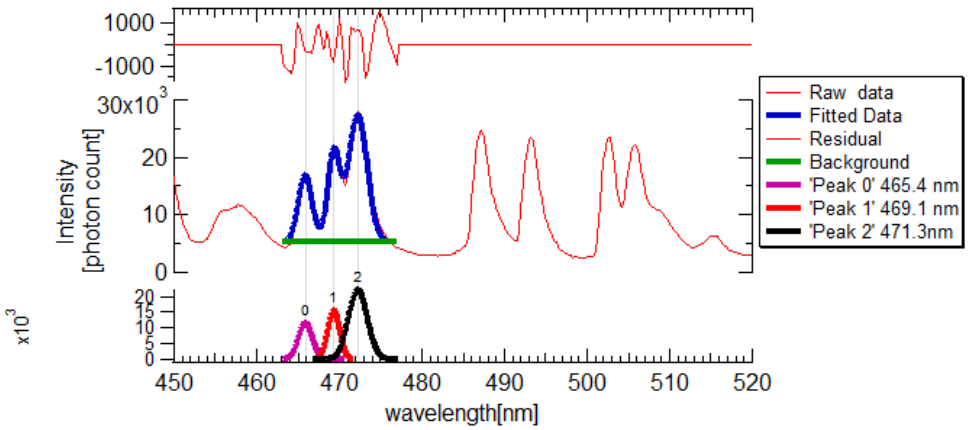

Figure 4.2: Figure showing the snap shot of the raw spectroscopic data and multi-peak fitting used to reconstruct 471.3 nm

inside Igor. Multi-peak fitting package reconstructs the individual spectral lines distinctly from the overlapping spectra using a specified function from the list. In figure 4.1, the distinct reconstructed spectral lines are shown in the bottom half of the figure. Figure

4.2 shows the raw spectroscopic snap shot showing wavelengths 706.5 nm and 728.1 nm. After analysing the raw spectroscopic data for the respective spectral lines, we calculated the radial profiles of their line integrated intensities across RT-1. From the radial profiles of the intensities, we calculated the radial profile of the line integrated intensity ratios sensitive either to electron temperature or electron density. Radial profiles for both the levitated and non-levitated cases . Moreover, for each case the radial profiles were taken with Ion Cyclotron Resonance Heating(ICRH)on and off, and the radial profiles were fitted to obtain the density and temperature profiles. Here it must be stated that although we used gauss fitting for all the cases, other fitting functions such as Lorentzian can also work very well. The line integrated intensity ratios for various plasma discharges- both for levitation and non-levitation- were measured, and then were used in concert the Abel Transform Model constructed in this research to obtain the corresponding temperature and density profile of the cold component.

4.2 Density and temperature profile in case of levitation

The line ratios $501.6nm(3^1P \rightarrow 2^1S)/471.3nm(4^3S \rightarrow 2^3P)$ have been used to determine the electron temperature and $492.2nm(4^1D \rightarrow 2^1P)/504.8nm(4^1S \rightarrow 2^1P)$ has been used to determine the density profile of the cold component. Below we have shown the radial

profiles of the respective line integrated intensities and the ratios for a pure helium gas discharge in case of levitation.

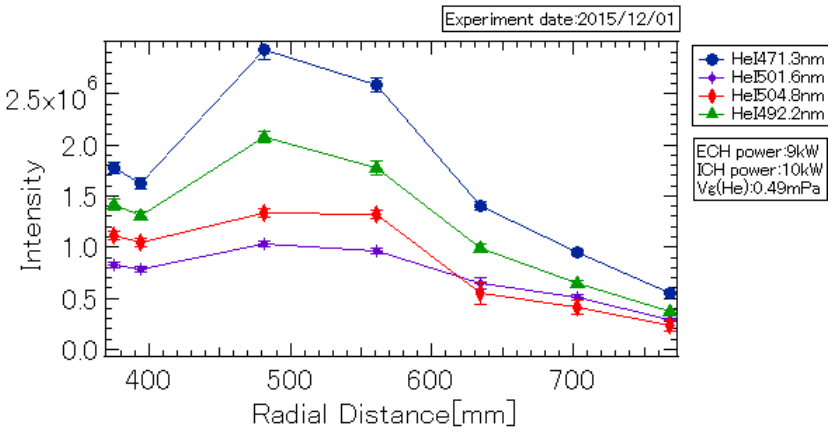

Figure 4.3: Radial profile of the various He I line integrated intensities for ICH off inside RT-1. The peak of the intensities is around r=0.48 m

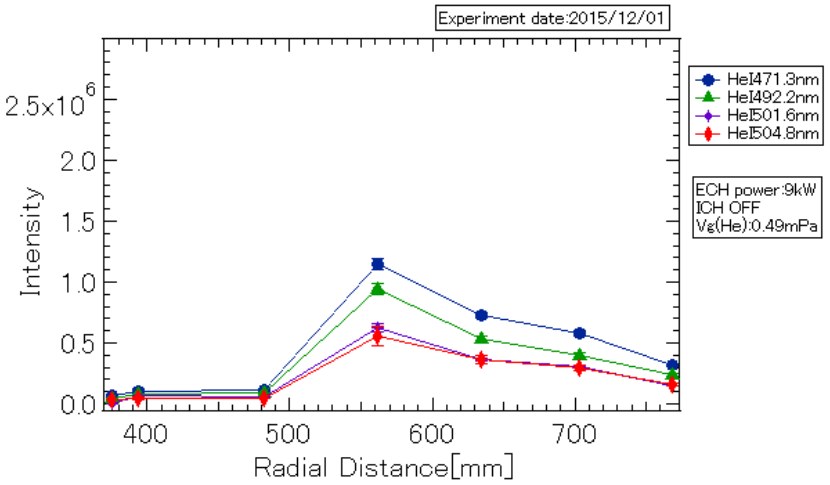

Figure 4.4: Radial profile of the various He I line integrated intensities for ICH On inside RT-1. The intensities here peak around 0.58 m

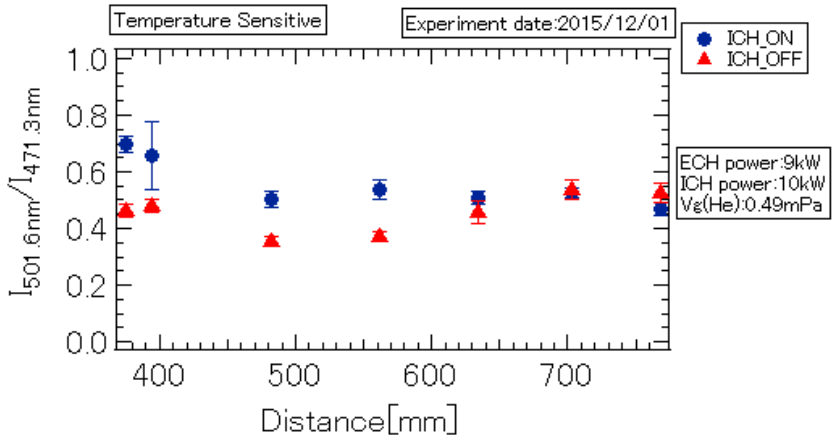

Figure 4.5: Radial profile of the temperature sensitive line ratio (I501.6nm/I471.3nm)across RT-1 for both ICH ON and OFF. Ratios show a double peak inclination, with the main peak occurring near coil and the secondary peak at the outer edges

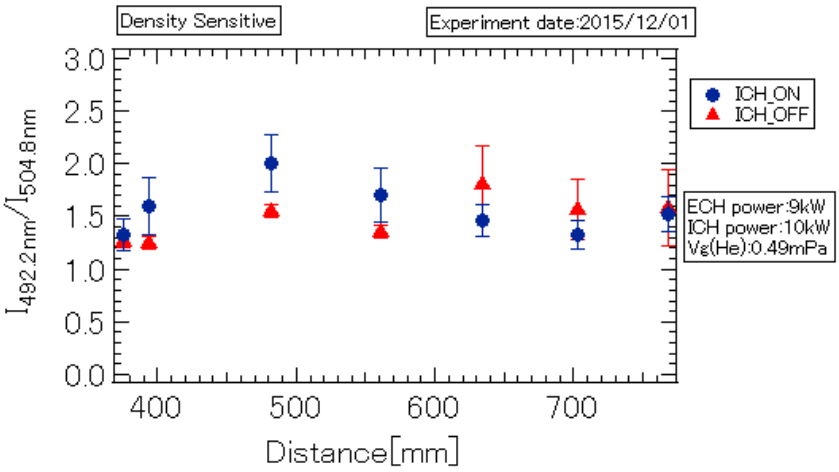

Figure 4.6: Radial profile of the density sensitive line ratio (I492.2nm/I504.6nm)across RT-1 for both ICH ON and OFF. ICH OFF shows double peaks, however ICH on shows only a single peak near 0.48 m.

The measurement was performed both with Ion Cyclotron Resonance Heating and without it, and then the results were compared to investigate any potential heating of the cold

component of electrons by Ion Cyclotron Heating. The fitting results for both the line intensity ratios, and the density and temperature profiles of the cold component have been evaluated and are presented below.

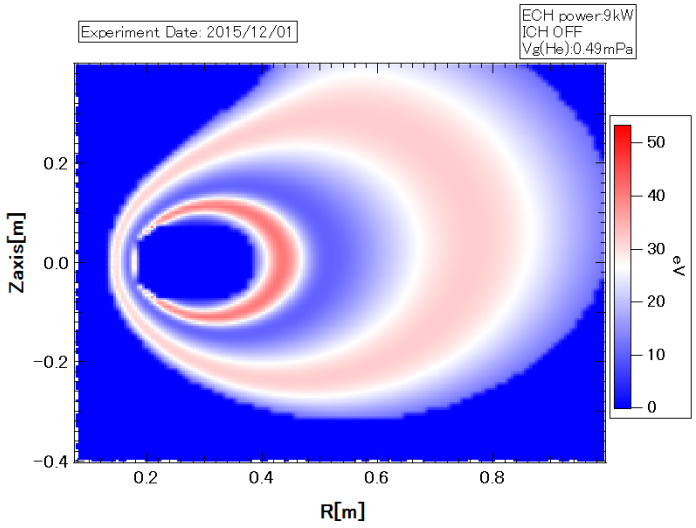

Figure 4.7: Electron temperature profile of the cold component over r-z plane for ICHOFF. Double peaks are visible, with the main occurring at the coil and the secondary peak on the periphery

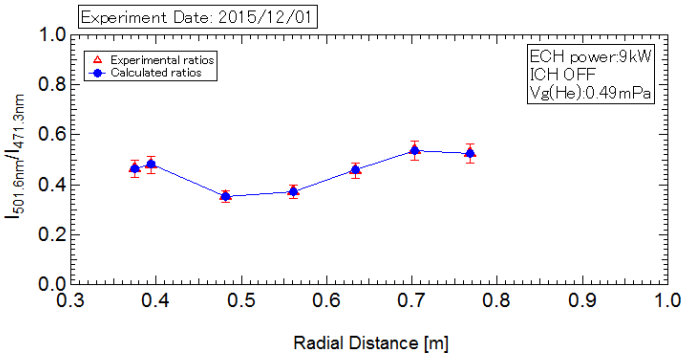

Figure 4.8: Figure showing the fitting for the temperature sensitive Intensity ratios in case of ICH OFF

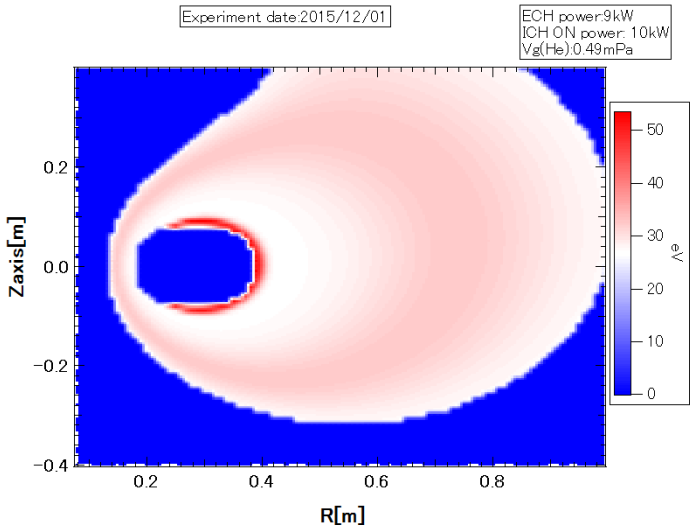

Figure 4.9: Electron temperature profile of the cold component over r-z plane for ICHON.Double peaks are visible, with the strong main peak occurring near the coil and the other weak broad peak occuringr_{z0}=0.7m

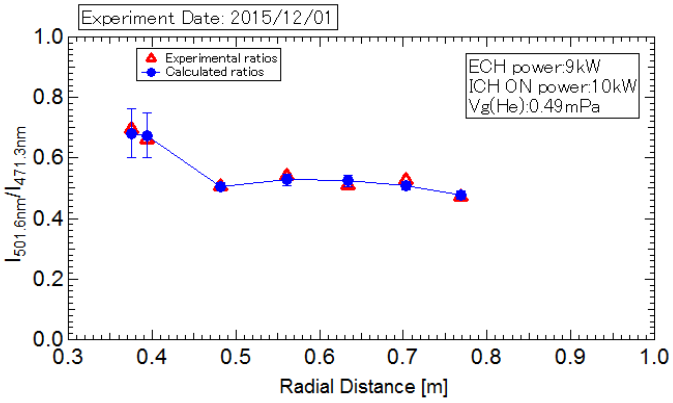

Figure 4.10: Figure showing the fitting for the temperature sensitive Intensity ratios in case of ICH ON

Te figures below show the fitting performed to the density ratios and the corresponding density profiles, both with ion cyclotron heating and without ion cyclotron heating.

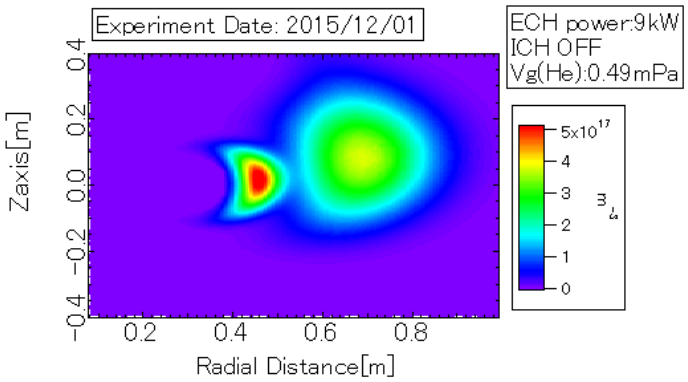

Figure 4.11: Electron density profile of the cold component over r-z plane for ICHOFF. Double peak are visible, with the main peak occurring at r_{z0}=0.42m, and secondary peak at r_{z0}=0.7 m

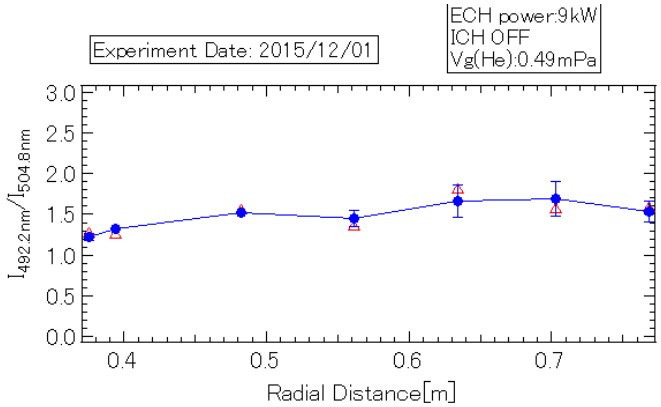

Figure 4.12: Figure showing the fitting for the density sensitive Intensity ratios in case of ICH OFF

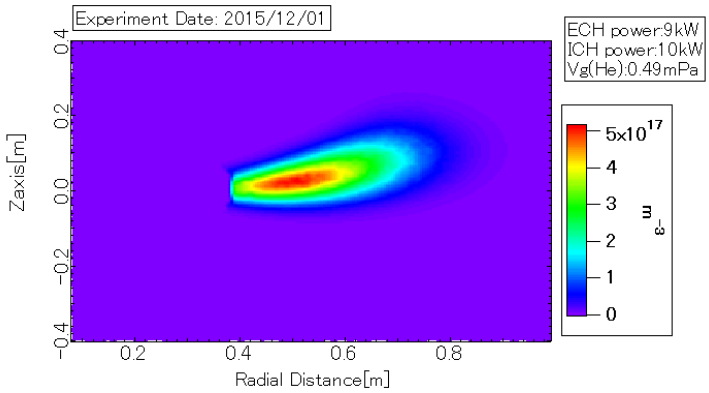

Figure 4.13: Electron density profile of the cold component over r-z plane for ICH On. The profile resembles a narrow strip with a broad peak centring at r_{z0}=0.43 m

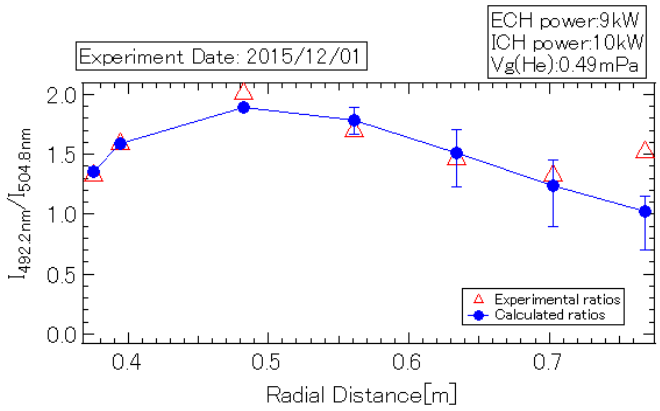

Figure 4.14: Figure showing the fitting for the temperature sensitive Intensity ratios in case of ICH ON

Figures 4.14 and 4.15 show the product of the density and temperature profiles for ICH On and ICH Off, respectively, and represent the energy distribution of the cold component of electron inside RT-1, both for ICH ON and ICH OFF. As can be seen from the comparison of figure 4.7 and 4.9, the heating affects of ICH on the cold component of electron are clearly visible. The region from 0.47 m to 0.58 m has a lower temperature when ICH is

off[fig.4.7] and a higher temperature when ICH is on[fig.4.8]. However, for both ICH ON and ICH OFF, the bulk electron temperature is flat for the central region, with electron temperature peaking near the coil. The electron density in case of ICH off shows double peaks; as can be seen from figure 4.11, the main peak occurs near the coil[R≈0.45m]and the second peak occurs in the central region- a little bit towards the outside[R≈0.69m].

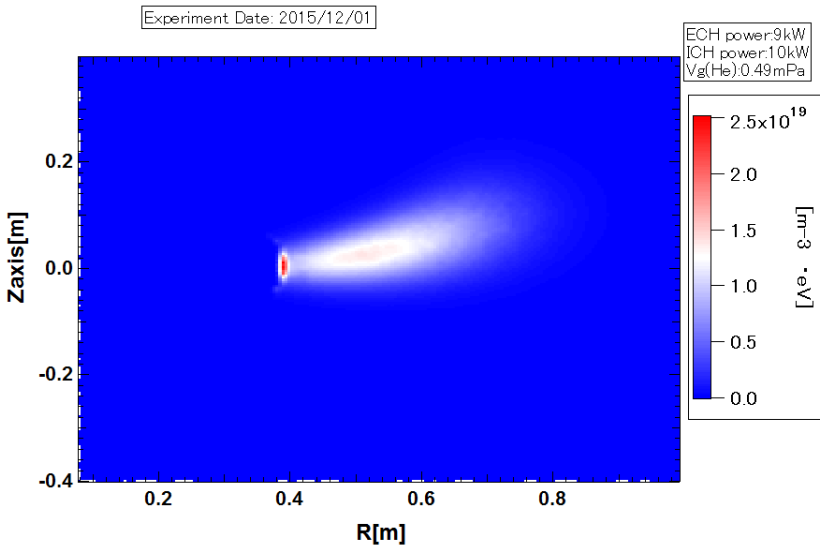

Figure 4.15: Pressure profile of the cold component of electron over r-z plane for ICH ON

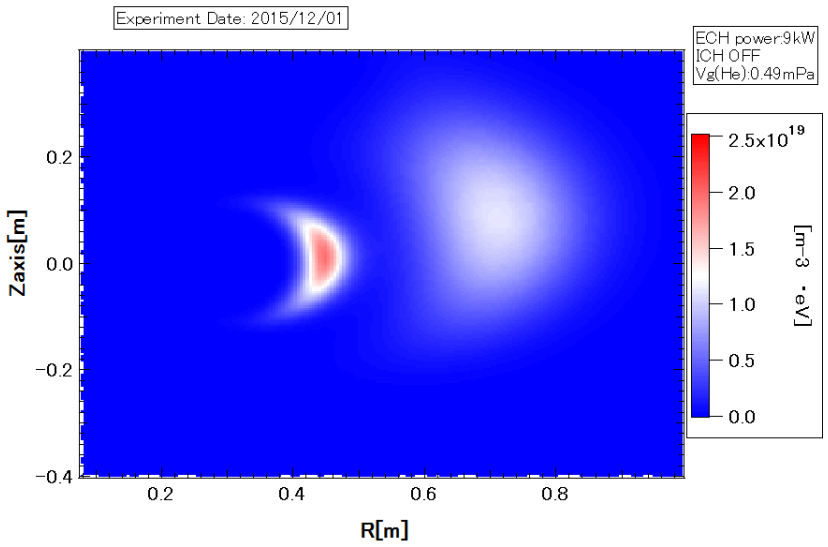

Figure 4.16: Pressure profile of the cold component of electron over r-z plane for ICH OFF

4.3 Density and temperature profile in case of support

The pair of ratios-501.6 nm/471.3 nm and 492.2 nm/504.6 nm- used to estimate the density and temperature profile of the cold component of electron in case of levitation were also used to determine the temperature and density profile of the cold component of electron in case of support.The radial profile of the various measured line integrated intensities- both for ICH On and Off- are shown below in figure 4.17 and 4.18. The radial profile of the density sensitive line integrated ratios both for ICH on and ICH off is shown in figure 4.19, and radial profile of the temperature sensitive line integrated ratios - both

for ICH on and ICH off is shown in figure 4.20.

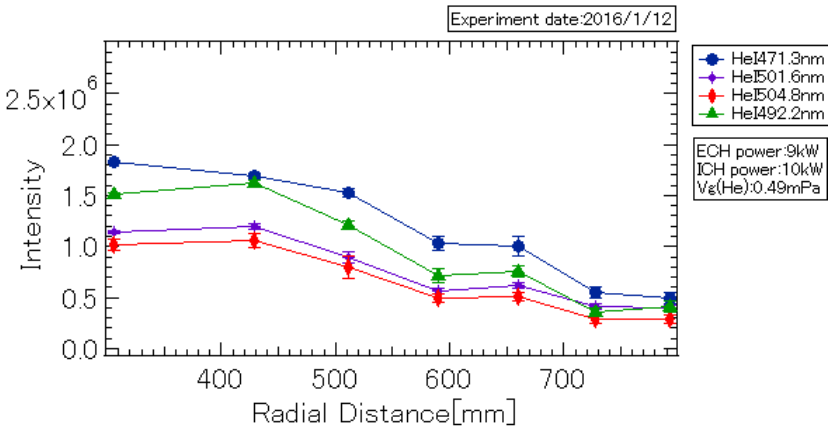

Figure 4.17: Radial profile of the various line integrated intensities inside RT-1 plasma for ICH Off. The peak of the line integrated line intensities occur around 0.3 m

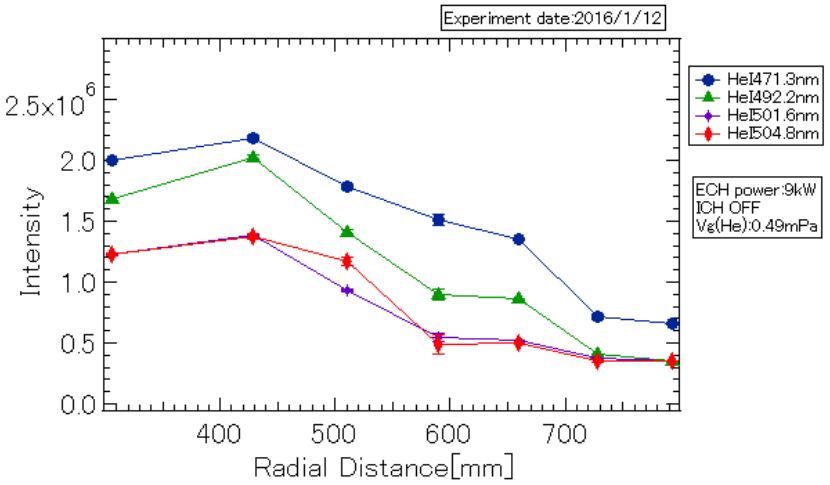

Figure 4.18: Radial profile of the various line integrated intensities inside RT-1 plasma for ICH on. The peak of the line integrated line intensities occur around 0.4 m

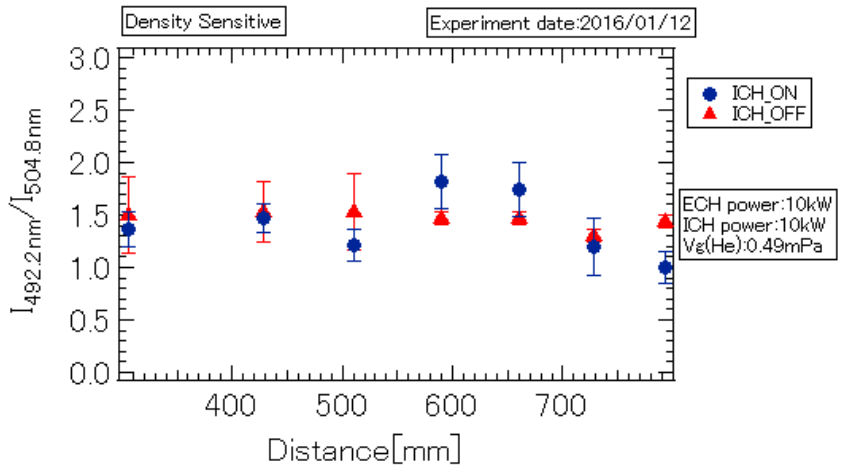

Figure 4.19: The radial profile of the density sensitive line intensity ratios both for ICH on and off. For ICH on the profile shows a double peak; however for ICH off it is almost flat

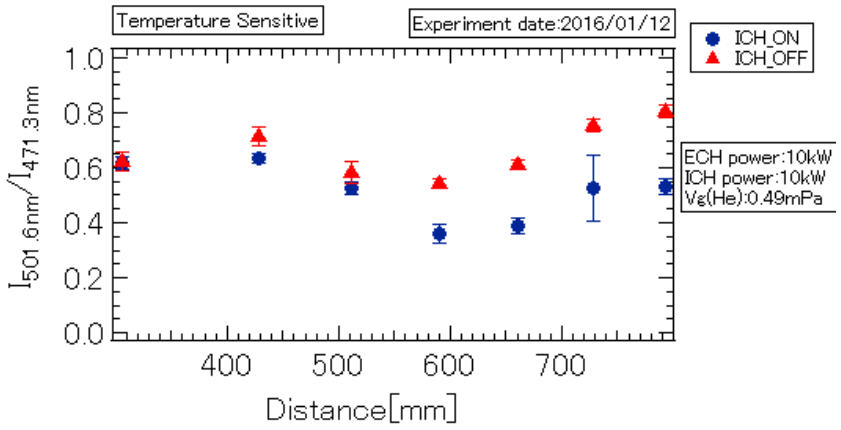

Figure 4.20: Radial profile of temperature sensitive line integrated intensity ratios. The ratios are higher in case of ICH OFF than in case of ICH on.

The line integrated intensities show a peak around 0.3 m when ICH is off and a peak at 0.4 m when ICH is on. The density sensitive line integrated ratios show a double peak for ICH on while show an almost flat profile for ICH OFF. The temperature sensitive ratios

501.5 nm/471.3 nm are higher in case of ICH off than in case of ICH ON. The results obtained after applying the Abel transform model to the experimentally measured line integrated intensity ratios are as follows.

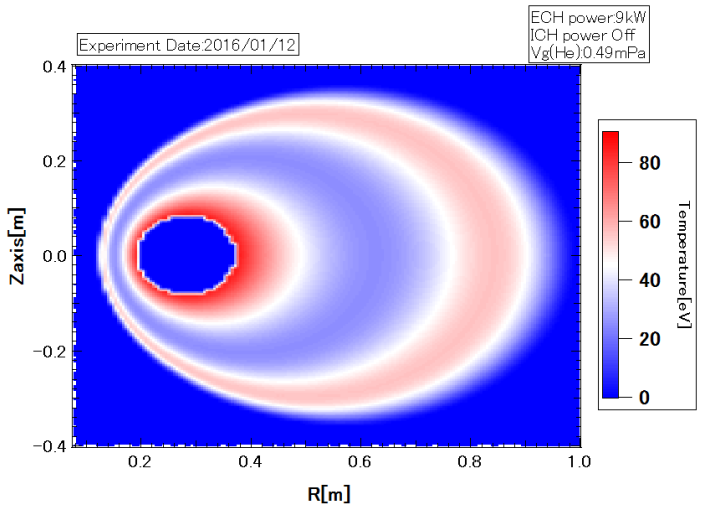

Figure 4.21: Electron temperature profile of the cold component over r-z plane for ICH OFF in case of no levitation. The profile has a double peak, with the main peak appearing near the coil and the other appearing around $r_{z0} \approx 0.7$ m

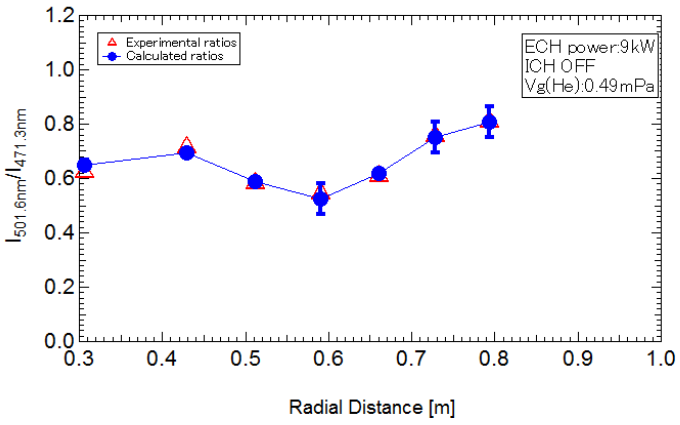

Figure 4.22: Figure showing the fitting results for the temperature profile obtained-in the figure above- for ICH off

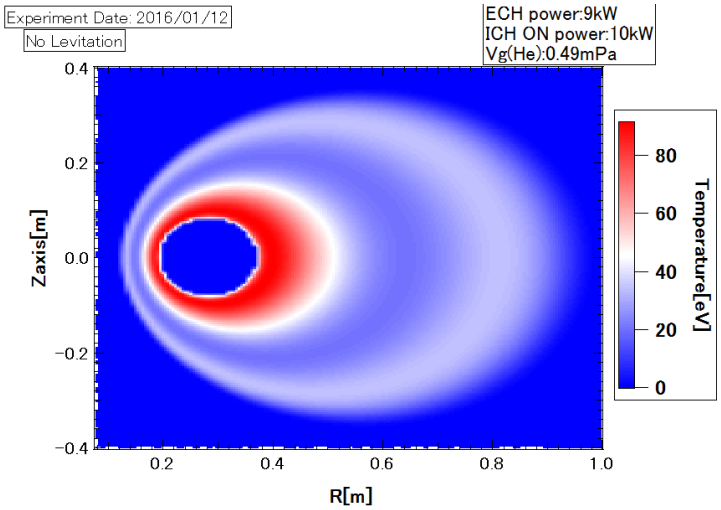

Figure 4.23: Electron temperature profile of the cold component over r-z plane for ICH ON in case of no levitation. The profile has a double peak, with the main peak appearing near the coil(around r_{z0} =0.42m) and a weak secondary peak appearing around r_{z0} ≈0.75m

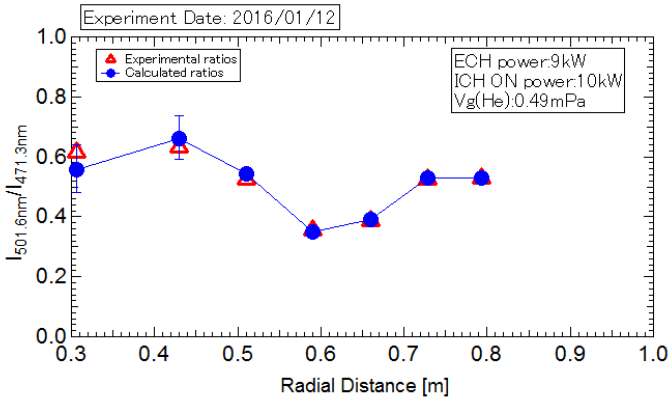

Figure 4.24: Figure showing the fitting results for the temperature profile obtained-in the figure above- for ICH on

Te figures below show the fitting performed to the density ratios and the corresponding density profiles, both with ion cyclotron heating and without ion cyclotron heating.

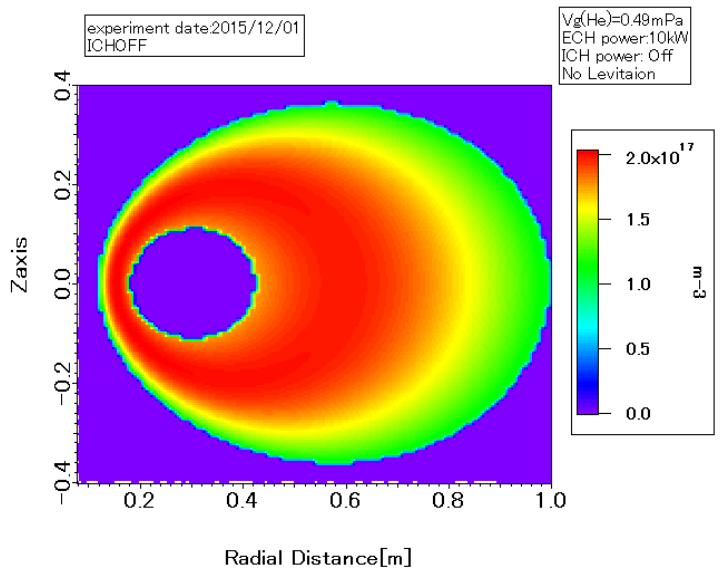

Figure 4.25: Electron density profile of the cold component over r-z plane for ICHOFF in case of no levitation.The density almost flat near the coil region and the bulk area.

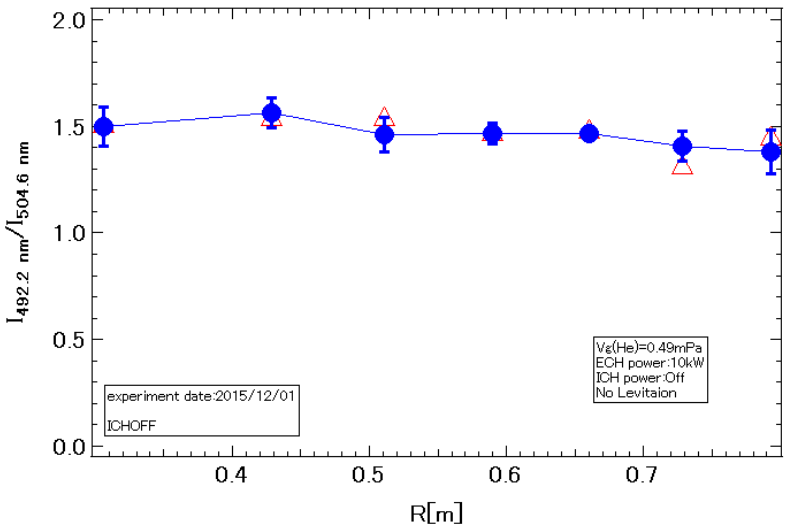

Figure 4.26: Figure showing the fitting applied to the density sensitive line integrated intensity ratios -in case of ICH OFF- in order to obtain the density profile obtained above.

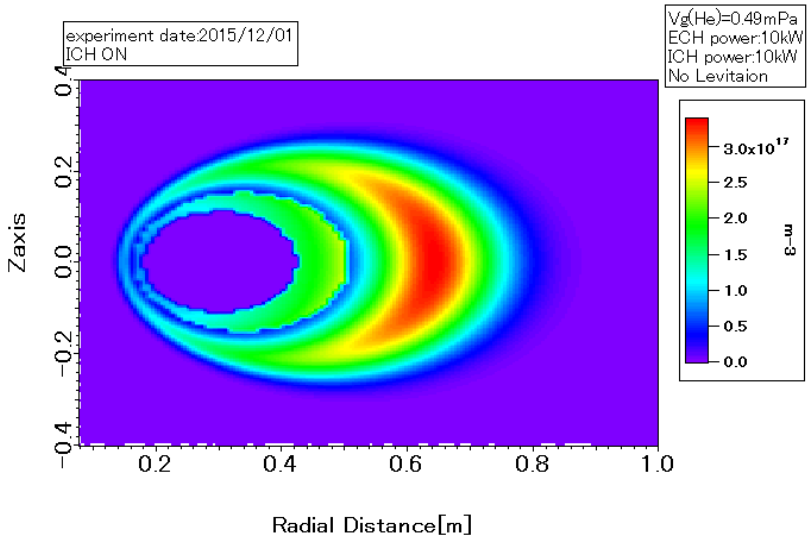

Figure 4.27: Electron density profile of the cold component over r-z plane for ICH ON. The profile shows a peak around r_{z0}=0.6 m

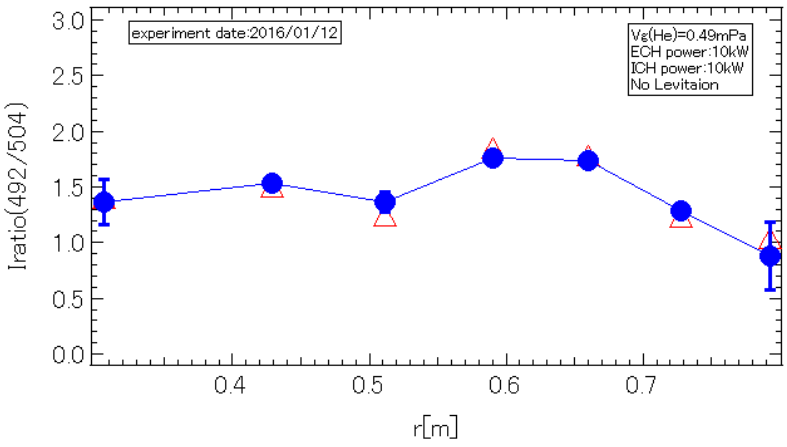

Figure 4.28: Figure showing the fitting applied to the density sensitive line integrated intensity ratios -in case of ICH On - in order to obtain the density profile obtained above.

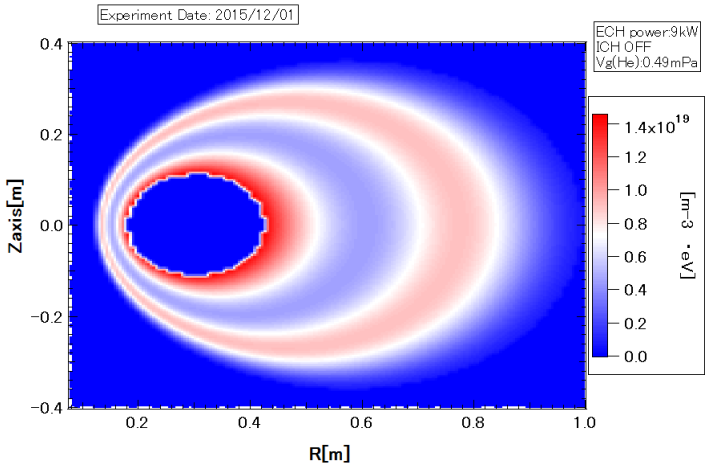

Figure 4.29: Figure showing the product of the temperature and density profile for ICH off in case of no levitation. The figure corresponds to the pressure or total energy of the cold component of electron inside RT-1 plasma. The main peak is near the coil and the secondary peak occurs around r_{z0}=0.7 m

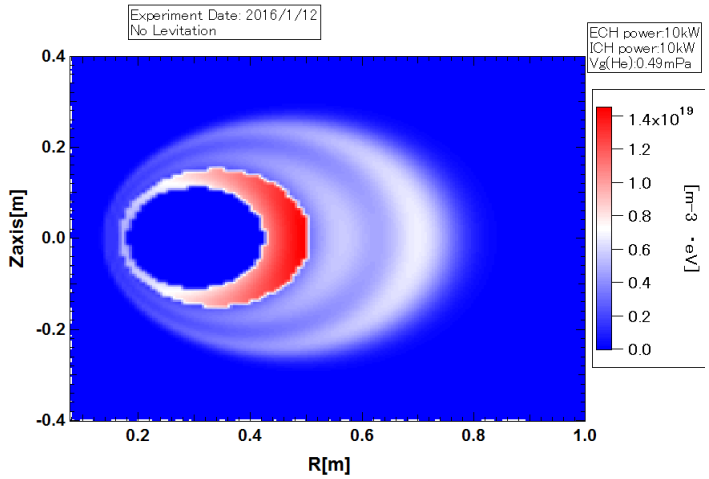

Figure 4.30: Figure showing the product of the temperature and density profile for ICH on in case of no levitation. The figure corresponds to the pressure or total energy of the cold component of electron inside RT-1 plasma. The main peak is near the coil and the two secondary peaks occurring at r_{z0}=0.56 m and r_{z0}=0.70 m

4.4 Discussion

Figure 4.17 and figure 4.18 shows the temperature and density comparison between the helium line intensity ratio method and the probe measurements, for the helium discharge investigated in this section. In case of levitation,as the probe can not be inserted very deep inside the plasma, we could only get data for two points inside RT-1. The temperatures obtained from the probe are lower than the temperatures, read from the temperature profile, obtained by the helium line intensity ratio method for the points for which the probe measurements were performed. For ICH ON, the density from the probe measurements was found higher than the densities from the density profile obtained by the helium line intensity ratio method. However, foe ICH OFF, it is found that the densities from the density profile is greater almost by an order 10 than the density from the probe measurements. In figure 4.19, we have compared the radial profile of the temperature of the cold component of electron with the radial profile of the CIII ion temperature for the equatorial plane,i.e. z=0. In fig.4.20, the radial profile of HEII ion temperature, on the equatorial plane, has been compared with the cold electron temperature component. The radial profile of the cold electron temperature component-for the equatorial axis- was extracted from the temperature profile of the cold electron component obtained from the helium intensity ratio method. The thick lines represent the temperature of the cold electron component, and the markers represent the ion temperature. It is quite evident from the figures, the temperature from the cold component of electron, for both ICH ON and

ICH OFF, is higher than the temperature of both the ions. The line averaged in RT-1, as mentioned in earlier chapter, is measured with the help of a set of 3 interferometers. The line averaged density is calculated from the density profile-obtained by the helium line intensity ratio method- along the lines of measurement for which the line averaged density has been calculated by interferometry. The figure 4.20, shows the ratio of the line averaged density measured by spectroscopy and the line averaged density measured by interferometry for r=700 mm(vertical),600 mm(vertical)and 450 mm(horizontal) from the central axis of RT-1. The ratio is greater than 1 except for r=450 mm when ICH is on. Although the ratio are greater than 1, they are pretty close to 1, and therefore, the line averaged density from helium line ratio method can be said to be in good agreement with the line averaged density measurements from the interferometry.

Ion Cyclotron Heating ON

R[mm],Z=120mm	T_e(Probe Measurement) [eV]	T_e(Helium Line Intensity ratio method) [eV]
900	12.7	29
950	9.266	28.3

Ion Cyclotron Heating OFF

R[mm],Z=120mm	T_e(Probe Measurement) [eV]	T_e(Helium Line Intensity ratio method) [eV]
900	11.233	22.27
950	6.69	17.68

Figure 4.31: Table showing comparison of the electron temperature of the cold component obtained from the Helium Line Intensity Ratio Method with that of the probe measurements. Probe data provided by M.Nakatsuka

Ion Cyclotron Heating ON

R[mm],Z=120mm	N_e(Probe Measurement) [m^{-3}]	N_e(Helium Line Intensity ratio method) [m^{-3}]
900	8.61718E+15	5.78E+15
950	2.76217E+15	1.19E+15

Ion Cyclotron Heating OFF

R[mm],Z=120mm	N_e(Probe Measurement) [m^{-3}]	N_e(Helium Line Intensity ratio method) [m^{-3}]
900	9.1949E+15	4.54E+16
950	2.47334E+15	1.98E+16

Figure 4.32: Table showing comparison of electron density of the cold component obtained from the Helium Line Intensity Ratio Method and the probe measurements. Probe data provided by M.Nakatsuka

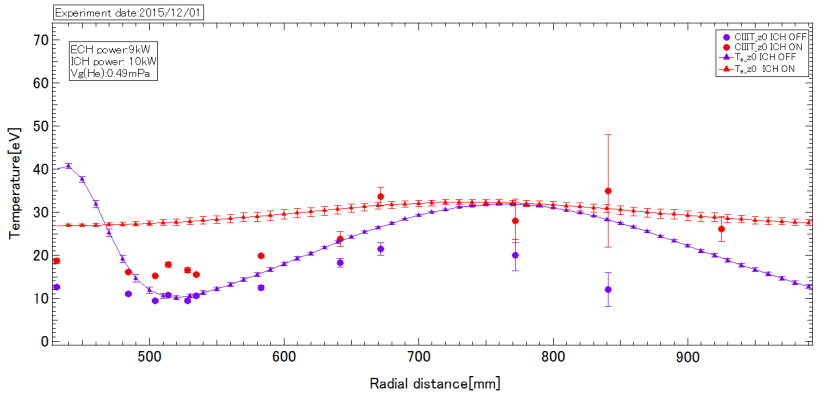

Figure 4.33: Comparison of electron temperature of the cold component with CIII ion temperature at z=0, for both ICH ON and ICH OFF scenarios. Ion temperature was provided by N.Takahashi

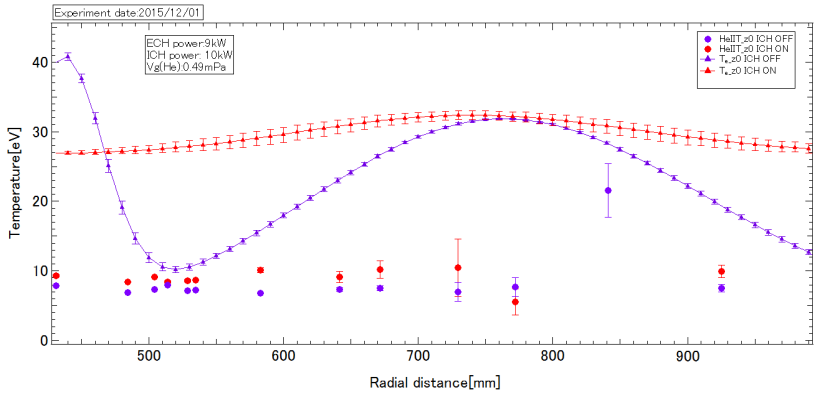

Figure 4.34: Comparison of electron temperature of the cold component with HeII ion temperature at z=0, for both ICH ON and ICH OFF scenarios. Ion temperature was provided by N.Takahashi

$$\frac{\textit{Line averaged } N_{e\ spectroscopy}}{\textit{Line averaged } N_{e\ interferometry}}$$

	R=450 mm	R=600 mm	R= 700 mm
ICHON	0.842211	2.13543	2.65309
ICH OFF	1.35029	2.58434	6.28697

Figure 4.35: Table showing comparison between the line integrated densities calculated from the density profile(obtained from line ratio method) and the ones estimated from interferometry

Chapter 5

Conclusion

In this research, we have successfully calculated the temperature and density profile of the cold component of electron in RT-1 plasma by helium I line intensity ratio method. The intensity of the desired lines were measured spectroscopically and ratios were calculated from them. $501.6nm/471.3nm$ helium I line intensity ratio was used to find the electron density and $492.2/504.8nm$ helium I line intensity ratio was used to find the electron temperature of the cold component. The ratios were chosen such that they were either a strong function of electron temperature or of electron density in the density regime of RT-1. In this research, results for a pure helium discharge were analysed and presented. First, the temperature and density profiles of the cold component of electron were calculated in case of levitation.The temperature profile shows an almost flat tendency for the bulk of the central region of plasma inside RT-1- both for ICH on and ICH OFF. In case of ICH OFF, a dip in temperatures occurs around 500 mm with the main peak of temperature

occurring at 400 mm.However, in case of ICH on, the heating affect is clearly visible in the region where a dip in temperatures is observed for ICH off; the temperature peak occurs near the coil. The fitting applied to the line integrated intensity ratios for estimating the temperature is quite both for ICH ON and Off.The density profile- both for ICH off and ICH on- is peaked near the coil. In case of ICH ON, the density profile is like a narrow elongated strip,with most of the plasma concentrated near the equatorial plane. However, in case of ICH off a secondary peak can also be seen around 700 mm. The fitting for the density sensitive line integrated ratios also went well,with only a little bit discrepancy at the periphery-in case of ICH ON. Next, the density and temperature profile of the cold component of electron in case of support were also estimated. In case of support, the temperature of the cold component of electron was estimated higher in case of ICH off than ICH on. In both the cases, a double peak of temperature was reported, with the main peak occurring near the coil and the secondary peak(low temperature peak)occurring at the outskirts of the central region in RT-1($r_{z0} \approx 0.7m$). The peak temperature of the cold component of electron in case of support was found to be 80 eV higher -in case of ICH off, and 30 eV higher -in case of ICH on-than the corresponding temperatures in case of levitation. The density-in case of ICH off-during support was found to be flat for most of the central region. However, the density in case Of ICH on showed double peak; the main density peak occurring around $r_{z0} \approx 0.62m$ and the secondary peak occurring around $r_{z0} \approx 0.4m$. The radial profile of the electron temperature at the equatorial

plane was extracted from the electron temperature profile and was compared with the temperature-of HII and CIII- at the equatorial plane. For both ICH ON and ICH off, the electron temperature of the cold component was found to be higher than the temperature of the respective ions. Line averaged densities measured using a a set of 3 interferometers were also compared with the line averaged densities calculated from the density profiles obtained from helium line intensity ratio method, and were found to be in close agreement. From various comparisons, it can be said that the helium line intensity ratio method can very reliably estimate the temperature and density of the cold component of electron in the central region of RT-1. However, in the periphery region of RT-1($r_{z0} \geqslant 0.850m$), the applicability of this method is questionable, as the helium line intensity ratios -in the density regime of that region-are intensive to electron temperature and density, and can not give a very accurate estimate of electron density and temperature of the cold component in that region. With the introduction of a revised population database for helium I excited levels, the reliability of the method formulated in this research can potentially be increased. Line integrated intensities for all the cases must be calculated properly,and a comparison with the experimentally measured line integrated intensities must be made. Moreover, using multiple density and temperature sensitive line ratios, in concert, can be a more accurate solution of density and temperature of the cold component of electron.

Chapter 6

Appendix

The pair of lines used in this research for the purpose of estimating the temperature and density profile of the cold component of electron was not used initially. In the nascent stages of this project, we used the pair $728.1nm(3^1S \rightarrow 2^1P)/706.5nm(3^3S \rightarrow 2^3P)$ to estimate the temperature profile of the cold component. Although, the aforementioned pair is a strong function of temperature in the density regime of RT-1, the fact that the density information regarding the cold component of electron,inside RT-1, is a prerequisite in estimating the temperature profile was not known. Most of the researches that have used helium line intensity ratio method for estimating electron temperature, either used it for plasmas with constant density, or used the temperature sensitive line integrated intensity ratios simultaneously with the density sensitive line integrated intensity ratios, to find the line integrated electron temperature and density. However, in this research we have applied Abel transform model both to the density sensitive and temperature

sensitive line integrated intensity ratios in an attempt to delineate the complete picture of the temperature and density of the cold component of electron inside RT-1. In our initial approach, we used the density profile, interpolated from the interferometry installed on RT-1, to estimate the temperature profile of the cold component of electron inside RT-1.The figure 6.1 show the density profile obtained form the interferometry that was used to estimate the electron temperature.

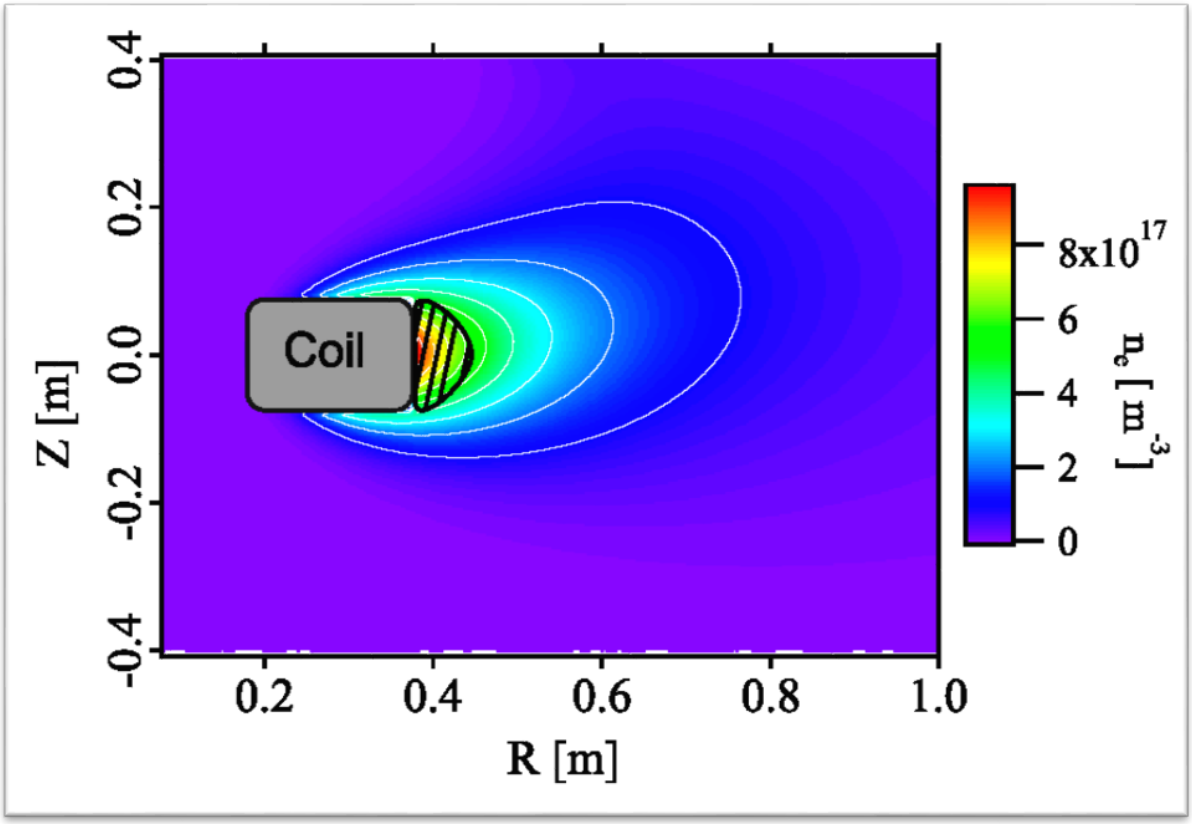

Figure 6.1: Poloidal cross section showing the density profile inside RT-1 obtained from interferometry. Figure provided by M.Nishiura

Databases of the emitting levels 3^1S and 3^3S corresponding to the neutral helium lines-

728.1 nm and 706.5 nm, were created using ADAS, and was used to perform a fitting on the experimentally measured $728.1nm(3^1S \rightarrow 2^1P)/706.5nm(3^3S \rightarrow 2^3P)$ line integrated intensity ratios, to obtain the temperature profile of the cold component of electron. Temperature was assumed as a function of magnetic flux as shown in the equation below:

$$T_e(\psi) = Af\left(\frac{\psi}{\psi_0} - 1\right)^B \left(1 - \frac{\psi}{\psi_1}\right)^C \tag{6.1}$$

Where $f = \left(\frac{B+C}{\psi_1 - \psi_0}\right)^{B+C}$ is the normalization factor. In order to verify the above assumption, initially the magnetic flux of a dipole magnetic field was used as a variable in the temperature function described above.Figures below show the fitting result and the temperature profile obtained from the fitting. For all the fittings performed there-

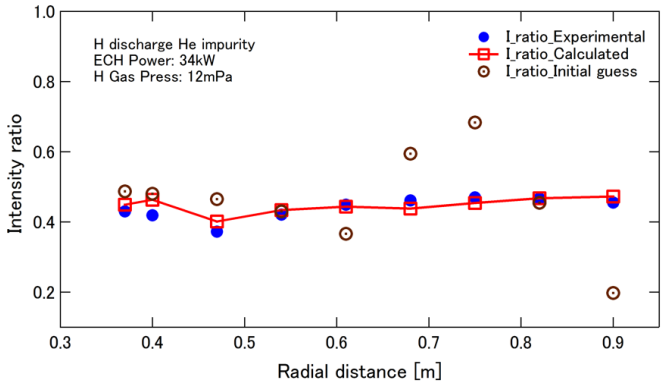

Figure 6.2: Figure showing the fitting applied to the experimentally measured 728.1 nm/706.5 nm line integrated intensity ratios.The blue markers represent the experimentally measured ratios and the red markers with the line represent the calculated line integrated ratio.

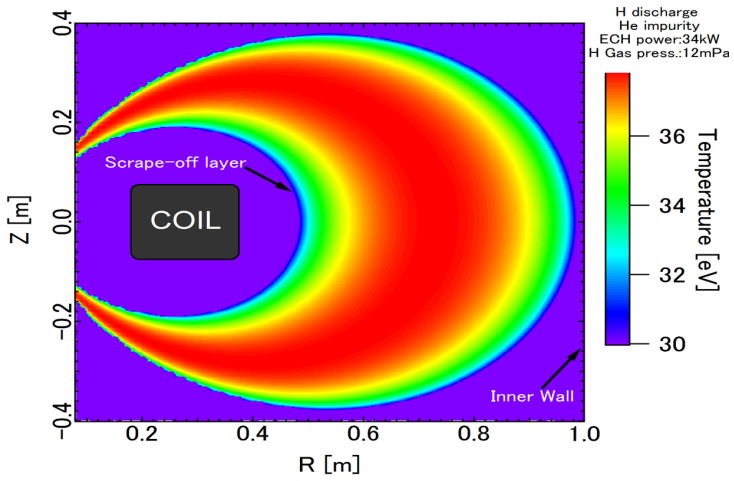

Figure 6.3: Temperature profile of the cold component of electrons corresponding for the fitting applied in figure 6.2.As can be seen, the temperature is quite flat in the central region

after, we used the magnetic flux inside RT-1 calculated from the code developed by H. Saitoh.Simultaneously, a second approach was also being considered in order to take into account the dip in the radial profile of the line integrated intensity ratios at 0.47 m. The approach was to consider the temperature to be a function of $B_\psi/B_{\psi,z=0}$ and not only ofψ. For the same experimentally measured line integrated line intensity ratios as above, temperature was considered as a function of $B_\psi/B_{\psi,z=0}$ and ψ as shown below:

$$T_e(\psi) = Af\left(\frac{\psi}{\psi_0} - 1\right)^B \left(1 - \frac{\psi}{\psi_1}\right)^C (B_\psi/B_{\psi,z=0})^E \tag{6.2}$$

The fitting results and the temperature profile- obtained from the above mentioned fitting- corresponding to two different scenarios is shown in figures 6.4,6.5,6.6 and 6.7 :

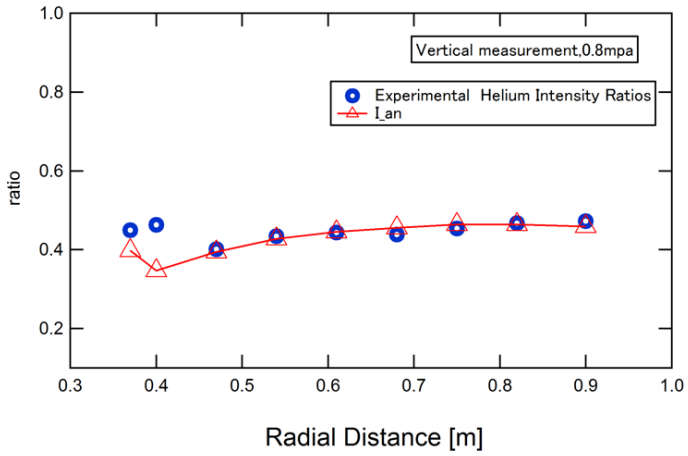

Figure 6.4: Figure showing the fitting applied to the experimentally measured 728.1 nm/706.5 nm line integrated intensity ratios, with $B_\psi/B_{\psi,z=0}$ having a negative power. The blue markers represent the experimentally measured ratios and the red markers with the line represent the calculated line integrated ratio.

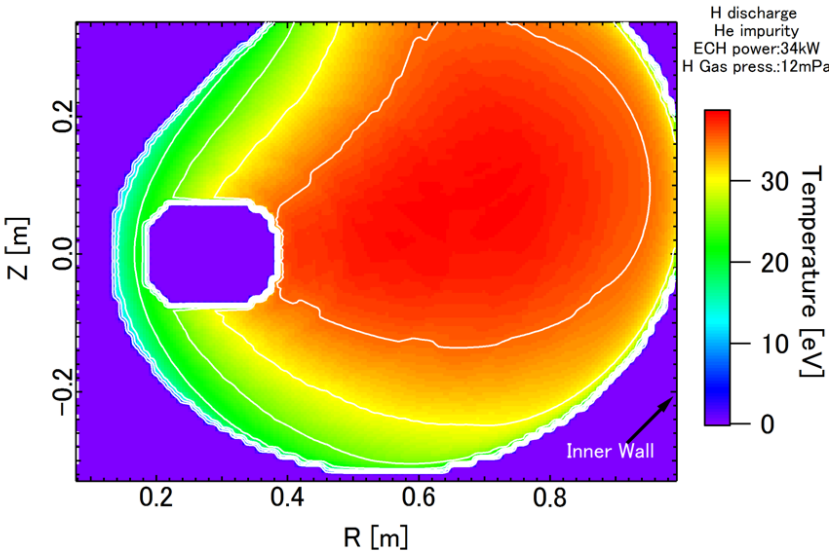

Figure 6.5: Temperature profile of the cold component of electrons corresponding for the fitting applied in figure 6.4($\psi = \psi_{RT-1}$).As can be seen, the temperature is flat in the central region, and ad goes alongψ towards the center the temperature decreases.

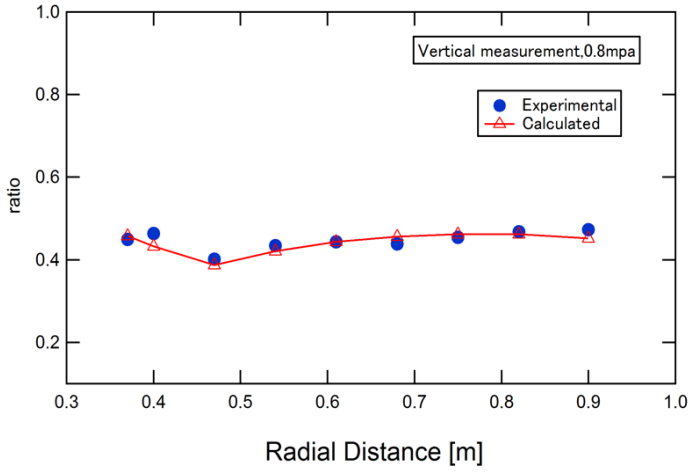

Figure 6.6: Figure showing the fitting applied to the experimentally measured 728.1 nm/706.5 nm line integrated intensity ratios, with $B_\psi/B_{\psi,z=0}$ having a positive power. The blue markers represent the experimentally measured ratios and the red markers with the line represent the calculated line integrated ratio.

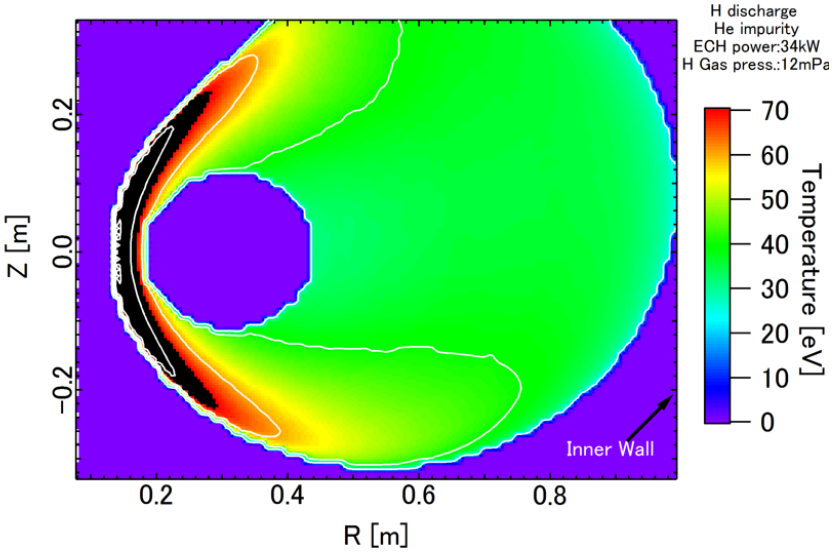

Figure 6.7: Temperature profile of the cold component of electrons corresponding for the fitting applied in figure 6.6.As can be seen, the temperature is flat in the central region. However as one travels along psi inwards the temperature increases. The black region represents the extrapolated values.

Figure 6.5 shows the temperature profile of the cold component when the power coefficient of $B_\psi/B_{\psi,z=0}$ is negative, and the temperature decreases as one moves inwards along ψ, whereas figure 6.7 shows the temperature profile when the power coefficient of $B_\psi/B_{\psi,z=0}$ is positive. Comparison with the horizontal spectroscopic measurement and initial probe measurements showed that the temperature near the ECRH- inner region of RT-1- can not be as high as predicted by the fitting where is T_e is given according to equation 6.2. Therefore, ultimately this fitting scenario was dropped, and the temperature expressed by equation 6.1 was used for fitting purposes from then on. After due deliberation, it was understood that simultaneous density and temperature measurements of the cold component of electron must be performed, if an accurate estimation of temperature is to be made.To that end, we decided to measure 667.8 nm/728.1 nm line intensity ratio simultaneously and used them in concert to estimate the density and temperature profile of the cold component of electron. The temperature and density are dependent on each other.Therefore, after every fitting, the fitted result was fed into the other for fitting.Figure 6.8 shows the fitting applied to 667.8 nm/728.1 nm line integrated intensity ratios and figure 6.9 shows the corresponding density profile obtained from it. The considered line intensity integrated ratio here is not very sensitive to the density in the density regime of RT-1 plasma, and therefore is not a good candidate. Figure 6.9 shows the fitting performed for temperature sensitive 728.1 nm/706.5 nm line integrated intensity ratios in case of support and figure 6.10 shows the temperature profile obtained from the ratios. As

is evident from the figures, the fitting for this ratio went exceedingly well. However, as the density ratio 667.8 nm/728.1 nm is not sensitive in this density regime, the temperature profile obtained is not very reliable. Therefore, in the end 492.2 nm/504.6 nm helium I line integrated intensity ratio was employed to find the density of the cold component of electron.

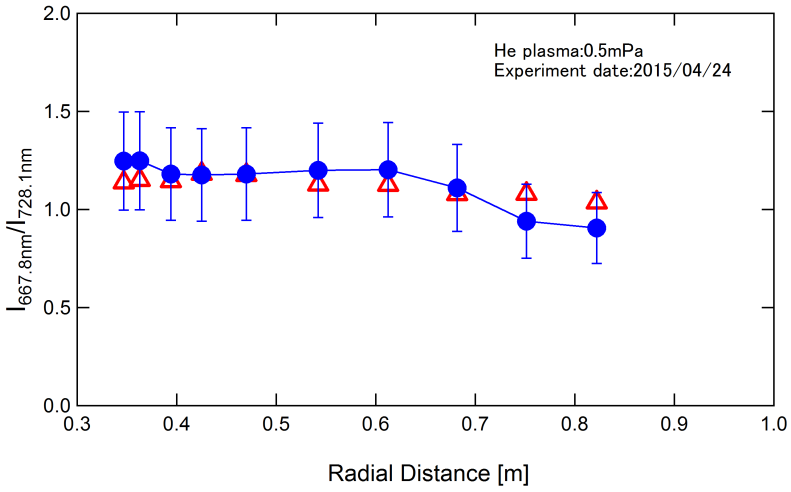

Figure 6.8: Figure showing the radial profile of 667.8 nm/728.1 nm line integrated density ratios and fitted result. This line ratio is not very density sensitive in the density regime of RT-1, and therefore the fitting is bad

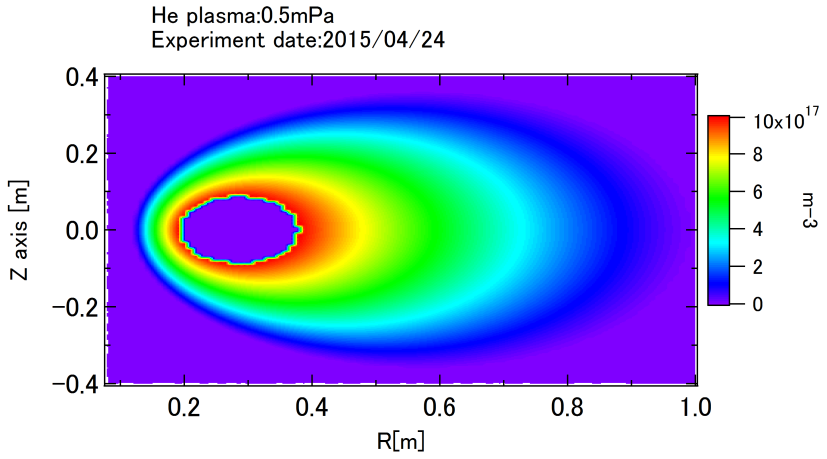

Figure 6.9: The density profile of the cold component during support in RT-1 obtained from 667.8 nm/728.1 nm line integrated ratio

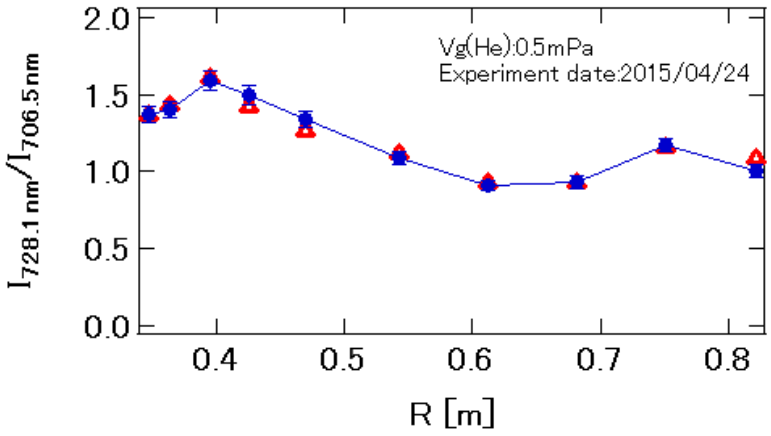

Figure 6.10: Figure showing the radial profile of 728.1 nm/667.8 nm line integrated temperature ratios and fitted result. This line ratio is sensitive to temperature in the density regime of RT-1, and therefore a good fitting has been achieved

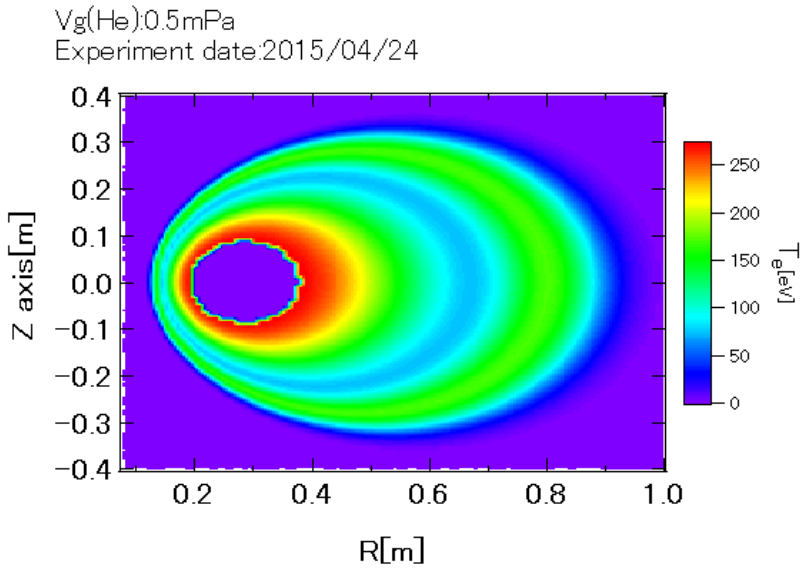

Figure 6.11: The temperature profile of the cold component during support in RT-1 obtained from 728.1/667.8 nm line integrated ratio for support. The profile has double peaks, with the main peak occurring near the coil,and the around 0.8 m with the dip occurring around 0.6 m

Bibliography

[1] Z.Yoshida et al., *Highβ Hot electron Plasma in Ring Trap 1(RT-1)*,22th IAEA Fusion Energy Conference,Switzerland, 2008 Ex/P5-28

[2] Z. Yoshida et al., *Magnetosphere-like Plasma Produced by Ring Trap 1 (RT-1) – A New Approach to High-Beta Confinement –*, 21th IAEA Fusion Energy Conference, China, 2006, IC/P7-14.

[3] H.Saitoh et al., *Measurement of a density profile of a hot-electron plasma in RT-1 with three-chord interferometry*, PHYSICS OF PLASMAS 22, 024503 (2015).

[4] Data obtained from T. Mushiake

[5] Y.Kawazura et al., *Observation of particle acceleration in laboratory magnetosphere*, Physics of Plasmas 22, 112503 (2015).

[6] S.Sasaki et al., *Helium I line Intensity ratios in a plasma for the diagnostics of the fusion edge plasma*,Rev. Sci. Instrum. 67, 3521 (1996)

[7] Z. Yoshida et al.*RT-1 project: magnetosphere-like plasma experiment*, Fusion Sci. Tech. 51 (2007), 29

[8] H.Saitoh et al., *High- plasma formation and observation of peaked density profile in RT-1*, 2011 IAEA, Vienna Nuclear Fusion, Volume 51, Number 6

[9] http://www.ppl.k.u-tokyo.ac.jp/research.html

[10] http://bwtek.com/spectrometer-part-4-the-optical-bench/

[11] R. F. Boivin1, J. L. Kline1 and E. E. Scime1, *Electron temperature measurement by a helium line intensity ratio method in helicon plasmas*,Phys. Plasmas 8, 5303 (2001)

[12] M.Goto, *Collisional Radiative model for neutral helium in plasma revisited*,Journal of Quantitative Spectroscopy & Radiative Transfer 76(2003)

[13] B.Schweer, et al., *Measurement of edge parameters in TEXTOR-94 at the low and high field side with atomic beams*, Journal of Nuclear Materials 266-269(1999)673-678

[14] J. L. Kline, E. E. Scime, P. A. Keiter, M. M. Balkey, and R. F. Boivin, Phys. Plasmas 6, 4767 (1999)

[15] http://open.adas.ac.uk/

[16] T.Fujimoto et al., *Ratio of Balmer line intensities resulting from dissociative excitation of molecular hydrogen in an ionizing plasma*,Journal of Applied Physics 66,2315(1989)

[17] T.Fujimoto et al., *New density diagnostic method based on emission line intensity ratio of Neutral hydrogen in an ionizing phase plasma*,NUCLEAR FUSION 28(7),2011

[18] W.L. Wiese and J.R. Fuhr, *Accurate Atomic Transition Probability for Hydrogen,Helium, and Lithium*, J.Phys.Chem.Ref. Data,Vol.38,No.3,2009

[19] S.S. Harilal et al., *Electron density and temperature measurements in a lase produced carbon plasma*, J. Appl. Phys. 82(5),1 September 1997

[20] Y.Andrew, et al., *Sensitivity of calculated neutral helium line intensities and their ratios to uncertainties in excitation rate coefficients*,Plasma Phys. Control Fusion 42(2000)301-307

[21] M.Goto, K.Sawada, *Determination of electron temperature and density at plasma edge in the Large Helical Device with opacity-incorporated helium collisional-radiative model*,Journal of Quantitative Spectroscopy & Radiative Transfer 137(2014)

[22] Ram Prakash et al., *Characterization of helium discharge cleaning plasmas in ADITYA tokamak using collisional-radiative model code*, Journal of applied physics 97,043301(2005)

[23] M.Goto, K.SAWADA, et al., *Emission Radiation of Hydrogen and Helium Atoms and Ions in plasma*, Contrib. Plasma Phys. 42(2002)2-4,212-217

[24] E de la Cal, *Application of passive spectroscopy to the He I line intensity ratio technique: a new tool for electron temperature and density measurement in fusion boundary plasma*, Plasma Phys. Control. Fusion 43(2001)

[25] S.Sasaki,M.Goto et al., *Line Intensity Ratios of Helium Atom in an Ionizing Plasma*, National Institute of Fusion Sciences

[26] Y. Ralchenko et al., *Electron-impact excitation and ionization cross-sections for ground state and excite helium atoms*,Atomic Data and Nuclear Data Tables 94(2008)

[27] N.K.Podder et al., *Helium line intensity ratio in microwave-generated plasmas*,Physics of plasma 11,5436(2004)

[28] M.Goto, T.Fujimoto, *Collisional-radiative for helium and its application to a tokamak plasma*, Fusion Engineering and design 34-35(1997)

[29] Niles Brenning, *Electron temperature measurements in low-density plasmas by helium spectroscopy*, Journal of Quantitative Spectroscopy and Radiative Transfer, Volume 24, Issue 4, Oct 1980

[30] H.Saitoh et al., *Long-Lived Pure Electron Plasma in Ring Trap-1, Plasma and fusion Research: Rapid Communications*, Volume 2, 045(2007)

[31] Z.Yoshida et al., *First plasma in the RT-1 device, Plasma and Fusion Research: Rapid Communications*, Volume 1,008

[32] H.Saitoh et al., *Formation of high-β plasma and stable confinement of toroidal electron plasma in Ring Trap 1*, Physics of plasmas 18,056102(2011)

[33] Y.Yano et al.,*Improvement of Field Accuracy and Plasma Performance in the RT-1 device*, Plasma and Fusion Research: Rapid communications, Volume 4,039(2009)

[34] S.Mizumaki et al., *Development of the Magnetically Floating Superconducting Dipoler in the RT-1 Plasma Device* IEEE Transactions on applied Superconductivity, Vol.16, No.2, June 2006

Chapter 7

Scientific Meetings

1. Ankur Kashyap, Zensho Yoshida, Masaki Nishiura, Yohei Kawazura, Yoshihisa Yano, Miyuri Yamasaki, Toshiki Mushiake, Izumi Murakami(NIFS)

   "Temperature measurement of the cold electron component using HE line intensity ratio method in RT-1 Plasma"

   JPS 2015 Annual meeting,24aAP-10, Waseda University(2015.3.24)

2. Ankur Kashyap, Zensho Yoshida, Masaki Nishiura, Yohei Kawazura, Yoshihisa Yano, Miyuri Yamasaki, Toshiki Mushiake, Izumi Murakami(NIFS)

   "Temperature and density profile of the cold electron component in RT-1 plasmas"

   JPS 2015 Autumn meeting,19aCN,OSAKA CITY University (2015.11.9)

3. Ankur Kashyap, Zensho Yoshida, Masaki Nishiura, Yohei Kawazura, Yoshihisa Yano, Miyuri Yamasaki, Toshiki Mushiake, Izumi Murakami(NIFS)

"Spectroscopic Measurement of the cold component of electron in ICH heating experiments on RT-1 Plasma"

Plasma spectroscopy Joint research Conference,National Institue of Fusion Science(2016.01.28)

Chapter 8

Acknowledgment

There are many people all across Japan-including friends, former classmates and my current lab members- whom I would like to earnestly thank for their constant support and motivation through this arduous journey of two years. I would ,first and foremost, like to express my deepest gratitude towards my Supervisor Professor Zensho Yoshida without whose esteemed guidance this research could not have been finished. His feedback to the results of my experiments and the degree of freedom he provides his students in conducting research, allowed me to finish this project in due time. I would also like to thank Assistant Professor M. Nishiura. M. Nishsiura is a great experimentalist, and his experience in the field of experimental plasma physics and deep insights into the experiments being conducted On RT-1, helped me in overcoming the obstacles I faced during the execution of the project. His valuable advice, not only on research but also on personal life, helped me a lot in thinking about my career. I am also very grateful to Mr. Kawazura for

his guidance in the field of spectroscopy and constant support in the development of the experimental set up. The long discussions regarding the line ratio method that I had with him also proved very beneficial in constructing the model employed here for estimating the temperature and density profile of the cold component. I am also grateful to Professor I. Murakami of the National Institute of Fusion Sciences for proving access to ADAS database from which the population densities of the emitting level of neutral helium were calculated. I am also thankful to other lab members of my lab- T. Mushiake, N.Takahashi and M. Nakatsuka- for the constant support they provided me in these two years. Finally, I would like to mention the names of some friends without whose emotional support these undulating journey could not have been made. I would like to thank my friends-Rusudan Kevkhishvili, Sato Naoki, Vivek Asokanand and Toshiki Mushiake- for the constant support, advice, and financial and emotional help they extended-when the journey became exceedingly tumultuous and scary. I will, very certainly, never forget the rich variegated experience I had in the Kashiwa campus of the University of Tokyo for my entire life.

This access to ADAS database- used in this research-was provided by National Institute of Fusion Science(NIFS).